

5-19-2021

# *Coxiella Burnetii* and Related Tick Endosymbionts Evolved from Pathogenic Ancestors

Amanda E. Brenner  
Portland State University, amanda.brenner@pdx.edu

Sebastián Muñoz-Leal  
Universidad de Concepción

Madhur Sachan  
Portland State University, madhur@pdx.edu

Marcelo B. Labruna  
Universidade de São Paulo

Rahul Raghavan  
Portland State University, rahul.raghavan@pdx.edu

Follow this and additional works at: [https://pdxscholar.library.pdx.edu/bio\\_fac](https://pdxscholar.library.pdx.edu/bio_fac)

 Part of the [Biology Commons](#)

Let us know how access to this document benefits you.

---

## Citation Details

Brenner, A. E., Muñoz-Leal, S., Sachan, M., Labruna, M. B., & Raghavan, R. (2021). *Coxiella burnetii* and related tick endosymbionts evolved from pathogenic ancestors. *Genome Biology and Evolution*, evab108. <https://doi.org/10.1093/gbe/evab108>

This Article is brought to you for free and open access. It has been accepted for inclusion in Biology Faculty Publications and Presentations by an authorized administrator of PDXScholar. Please contact us if we can make this document more accessible: [pdxscholar@pdx.edu](mailto:pdxscholar@pdx.edu).

1  
2  
3 **1** *Coxiella burnetii* and related tick endosymbionts evolved from pathogenic ancestors  
4  
5  
6  
7  
8  
9  
10  
11  
12  
13  
14  
15  
16  
17  
18  
19  
20  
21  
22  
23  
24  
25  
26  
27  
28  
29  
30  
31  
32  
33  
34  
35  
36  
37  
38  
39  
40  
41  
42  
43  
44  
45  
46  
47  
48  
49  
50  
51  
52  
53  
54  
55  
56  
57  
58  
59  
60

2

3 Amanda E. Brenner<sup>1</sup>, Sebastián Muñoz-Leal<sup>2</sup>, Madhur Sachan<sup>1</sup>, Marcelo B. Labruna<sup>3</sup>,

4 Rahul Raghavan<sup>1,4\*</sup>

5

6 <sup>1</sup>Department of Biology and Center for Life in Extreme Environments, Portland State  
7 University, Portland, OR 97201, USA.

8 <sup>2</sup>Departamento de Patología y Medicina Preventiva, Facultad de Ciencias Veterinarias,  
9 Universidad de Concepción, Chillán, Ñuble, Chile.

10 <sup>3</sup>Departamento de Medicina Veterinária Preventiva e Saúde Animal, Faculdade de  
11 Medicina Veterinária e Zootecnia, Universidade de São Paulo, São Paulo, Brazil.

12 <sup>4</sup> Department of Biology and South Texas Center for Emerging Infectious Diseases, The  
13 University of Texas at San Antonio, San Antonio, TX 78249, USA.

14

15 \*Author for correspondence:

16 Rahul Raghavan | Phone: 210-458-7016 | Email: [rahul.raghavan@utsa.edu](mailto:rahul.raghavan@utsa.edu)

17

18

© The Author(s) 2021. Society for Molecular Biology and Evolution.

This is an Open Access article distributed under the terms of the Creative Commons Attribution License

(<http://creativecommons.org/licenses/by/4.0/>), which permits unrestricted reuse, distribution, and reproduction in any medium, provided the original work is properly cited.

19 **ABSTRACT**

20 Both symbiotic and pathogenic bacteria in the family Coxiellaceae cause morbidity and  
21 mortality in humans and animals. For instance, *Coxiella*-like endosymbionts (CLEs)  
22 improve the reproductive success of ticks — a major disease vector, while *Coxiella*  
23 *burnetii* causes human Q fever, and uncharacterized coxiellae infect both animals and  
24 humans. To better understand the evolution of pathogenesis and symbiosis in this  
25 group of intracellular bacteria, we sequenced the genome of a CLE present in the soft  
26 tick *Ornithodoros amblus* (CLEOA) and compared it to the genomes of other bacteria in  
27 the order Legionellales. Our analyses confirmed that CLEOA is more closely related to  
28 *C. burnetii*, the human pathogen, than to CLEs in hard ticks, and showed that most  
29 clades of CLEs contain both endosymbionts and pathogens, indicating that several CLE  
30 lineages have evolved independently from pathogenic *Coxiella*. We also determined that  
31 the last common ancestor of CLEOA and *C. burnetii* was equipped to infect  
32 macrophages, and that even though horizontal gene transfer (HGT) contributed  
33 significantly to the evolution of *C. burnetii*, most acquisition events occurred primarily  
34 in ancestors predating the CLEOA-*C. burnetii* divergence. These discoveries clarify the  
35 evolution of *C. burnetii*, which previously was assumed to have emerged when an  
36 avirulent tick endosymbiont recently gained virulence factors via HGT. Finally, we  
37 identified several metabolic pathways, including heme biosynthesis, that are likely  
38 critical to the intracellular growth of the human pathogen but not the tick symbiont,

1  
2  
3  
4  
5  
6  
7  
8  
9  
10  
11  
12  
13  
14  
15  
16  
17  
18  
19  
20  
21  
22  
23  
24  
25  
26  
27  
28  
29  
30  
31  
32  
33  
34  
35  
36  
37  
38  
39  
40  
41  
42  
43  
44  
45  
46  
47  
48  
49  
50  
51  
52  
53  
54  
55  
56  
57  
58  
59  
60

39 and show that the use of heme analog is a promising approach to controlling *C. burnetii*

40 infections.

41

Downloaded from <https://academic.oup.com/gbe/advance-article/doi/10.1093/gbe/evab108/6278299> by guest on 26 May 2021

1  
2  
3 42 **Key words:** Coxiella, tick, endosymbiont, pathogen, heme  
4  
5

6 43  
7

8 44 **SIGNIFICANCE**  
9

10  
11 45 Coxiellae are enigmatic intracellular bacteria that adversely affect human and animal  
12  
13  
14 46 health, but their evolutionary origins and intracellular biology are not clearly  
15  
16  
17 47 understood. Here, by sequencing the first genome of a soft-tick endosymbiont, and  
18  
19  
20 48 combining this information with phylogenetic and phylogenomic analyses, we show  
21  
22 49 that endosymbiotic coxiellae evolved from pathogenic ancestors, and that the human  
23  
24  
25 50 pathogen *Coxiella burnetii* evolved from a preexisting pathogen — not from an avirulent  
26  
27  
28 51 tick endosymbiont as previously assumed. Additionally, having the genome of a closely  
29  
30  
31 52 related non-pathogen allowed us, for the first time, to perform in-depth comparative  
32  
33 53 genomic analyses, which identified several metabolic processes that are likely critical to  
34  
35  
36 54 *C. burnetii*'s intracellular growth and virulence. Knowledge gained from this study, in  
37  
38  
39 55 addition to helping us better understand the evolution of coxiellae, should hasten the  
40  
41  
42 56 development of novel therapies to control Q fever and could be applied to controlling  
43  
44 57 the spread of ticks.  
45

46 58  
47  
48  
49  
50  
51  
52  
53  
54  
55  
56  
57  
58  
59  
60

## 59 INTRODUCTION

60 A bacterium's genome size and gene content signal both the degree of its dependence  
61 on the host and the length of the bacterium-host relationship. For example, a bacterium  
62 that has established a long-term, obligate symbiosis would have a tiny genome filled  
63 with protein-coding genes (Wernegreen et al. 2000). Conversely, the genome of a  
64 bacterium that is in early stages of symbiosis is usually large and contains numerous  
65 pseudogenized genes, which, as the relationship progresses, would eventually be lost,  
66 resulting in a tiny genome (Moran 2002; McCutcheon and Moran 2011). The genomes of  
67 *Coxiella*-like endosymbionts (CLEs) found in ticks (Acari: Ixodida) fall into both  
68 categories: Some ticks, e.g., *Amblyomma americanum* and *A. sculptum*, contain small-  
69 genomed CLEs (~0.6 Mbp) that have few pseudogenes, indicating that they represent an  
70 ancient lineage of tick endosymbionts (Smith et al. 2015). In contrast, CLEs in  
71 *Rhipicephalus turanicus* (CRT), and *R. sanguineus* have large genomes (~1.7 Mbp) filled  
72 with pseudogenes, denoting that the bacteria are in early stages of symbioses (Gottlieb  
73 et al. 2015; Tsementzi et al. 2018). While most ticks contain CLEs, a few have *Francisella*-  
74 like endosymbionts (FLEs) (Gerhart et al. 2016, 2018; Duron et al. 2017). All FLEs  
75 studied to date have large genomes (~1.5 Mbp) with hundreds of pseudogenes,  
76 including inactivated virulence genes, indicating that FLEs evolved recently from  
77 pathogenic ancestors (Gerhart et al. 2016, 2018; Duron et al. 2018). Irrespective of their  
78 age, CLEs and FLEs improve the reproductive fitness of their hosts by likely providing

1  
2  
3 79 metabolites missing in vertebrate blood, ticks' sole nutritional source (Gottlieb et al.  
4  
5  
6 80 2015; Smith et al. 2015; Gerhart et al. 2016, 2018; Duron et al. 2017, 2018; Tsementzi et al.  
7  
8  
9 81 2018).

10  
11 82 *C. burnetii*, the causative agent of human Q fever, has also been detected in ticks;  
12  
13  
14 83 in fact, the intracellular pathogen was first isolated from hard ticks *Dermacentor*  
15  
16  
17 84 *andersoni* and *Haemaphysalis humerosa* (Cox 1938; Smith and Derrick 1940). In addition,  
18  
19  
20 85 transstadial transmission and fecal excretion of *C. burnetii* occur in laboratory-raised  
21  
22  
23 86 ticks (Eldin et al. 2017; Körner et al. 2020). However, it is not clear whether ticks play  
24  
25  
26 87 any meaningful role in the natural spread of *C. burnetii* (Duron et al. 2015b); instead, Q  
27  
28  
29 88 fever generally occurs following inhalation of *C. burnetii*-contaminated aerosols  
30  
31  
32 89 originating from infected farm animals (Maurin and Raoult 1999; Eldin et al. 2017).  
33  
34  
35 90 Within the human lungs, *C. burnetii* infects alveolar macrophages and generates a large  
36  
37  
38 91 replicative vacuole, termed the *Coxiella*-containing vacuole (CCV), by subverting host  
39  
40  
41 92 responses through a Dot/Icm Type IVB secretion system (T4BSS). This secretion system  
42  
43  
44 93 is essential to the pathogenicity of both *C. burnetii* and *Legionella pneumophila*, the two  
45  
46  
47 94 established pathogens in the order Legionellales (Segal et al. 1999; Chen et al. 2010;  
48  
49  
50 95 Beare et al. 2011; Newton et al. 2014; Burstein et al. 2016). Genes for T4BSS, which  
51  
52  
53 96 evolved from conjugation machinery, have spread across the bacterial kingdom via  
54  
55  
56 97 horizontal gene transfer (HGT), a process through which organisms gain foreign genes,  
57  
58  
59  
60

1  
2  
3 98 allowing them to quickly adapt to a new environment (Ochman et al. 2000; Lerat et al.  
4  
5  
6 99 2005).

7  
8  
9 100 The closest relatives of *C. burnetii* are CLEs present in ticks (Almeida et al. 2012;  
10  
11 101 Duron et al. 2015a; Smith et al. 2015), leading to the notion that the human pathogen  
12  
13  
14 102 emerged when an avirulent tick endosymbiont gained pathogenicity genes, probably  
15  
16  
17 103 via HGT (Duron et al. 2015a; Gerhart et al. 2016). Contrary to this hypothesis, by  
18  
19  
20 104 sequencing the genome of a CLE in *Ornithodoros amblus* (henceforth referred to as  
21  
22 105 CLEOA), we show that a common virulent ancestor gave rise to both *C. burnetii* and  
23  
24 106 CLEOA. The potentially-pathogenic ancestor contained genes for most virulence  
25  
26  
27 107 factors, including T4BSS, indicating that the erstwhile bacterium was likely capable of  
28  
29  
30 108 infecting mammalian macrophages. In CLEOA, homologs of most virulence-associated  
31  
32  
33 109 genes have been rendered non-functional, but genes for B vitamin and cofactor  
34  
35  
36 110 biosynthesis have been retained, suggesting that a virulent bacterium has morphed into  
37  
38  
39 111 a nutrient-provisioning tick endosymbiont. In a similar fashion, we found that several  
40  
41 112 other tick endosymbionts likely evolved from pathogenic ancestors, indicating that  
42  
43  
44 113 pathogen-to-endosymbiont transformation is widespread across ticks. Finally, by  
45  
46  
47 114 inhibiting *C. burnetii* growth using a synthetic analog of heme, a metabolite produced  
48  
49 115 by *C. burnetii* but not by CLEOA, we demonstrate how knowledge gained through  
50  
51  
52 116 comparative genomics could be applied to developing novel strategies to control Q  
53  
54  
55 117 fever, which is difficult to treat with currently available antibiotics.



118

119 **RESULTS**120 **CLEOA arose from a pathogenic ancestor**

121 Phylogenetic trees based mainly on 16S rDNA have previously indicated that the  
122 closest relatives of *C. burnetii* are CLEs present in *Ornithodoros* and *Argas* soft ticks  
123 (family Argasidae) (Almeida et al. 2012; Duron et al. 2015a; Smith et al. 2015); however,  
124 all CLE genomes available to date are from CLEs in hard ticks (family Ixodidae)  
125 (Gottlieb et al. 2015; Smith et al. 2015; Tsementzi et al. 2018; Guizzo et al. 2017),  
126 stymieing earlier efforts to understand *C. burnetii* evolution. Here, by sequencing the  
127 first soft-tick CLE genome, we were able to build a more definitive phylogenomic tree,  
128 which confirmed that CLEOA is a sister taxon of *C. burnetii* (**Fig. 1**; Supplemental Table  
129 S1). In addition, the presence of pseudogenized T4BSS genes in CLEOA indicates that  
130 the tick-symbiont evolved from a pathogenic ancestor with a functional T4BSS (**Fig. 2**;  
131 Supplemental Table S2).

132 To resolve the ancestry of pathogenicity in Legionellales we determined the  
133 prevalence of T4BSS, which is an essential virulence factors in this group of bacteria that  
134 includes human pathogens (*C. burnetii* and *L. pneumophila*), opportunistic pathogens  
135 (*Rickettsiella*), and symbionts (CLEs). Our analyses revealed that the secretion system is  
136 intact in all members of this order with the exception of CLEs, which only contained  
137 remnants of the T4BSS (**Figs. 1, 2**). The most parsimonious explanation for this phyletic

1  
2  
3 138 pattern is that T4BSS was present in the common ancestor of all Legionellales and was  
4  
5  
6 139 later lost in lineages that gave rise to CLEs, including CLEOA.  
7

8  
9 140

### 11 141 **Multiple CLEs have evolved from pathogens**

12  
13  
14 142 *Coxiella* detected in ticks are classified into four clades, three of which contain  
15  
16  
17 143 intermingled pathogens and endosymbionts (**Fig. 3**; Supplemental Table S3; Duron et  
18  
19  
20 144 al. 2015a). Clade A includes *C. burnetii* — the human pathogen, and CLEOA, which  
21  
22 145 arose from a pathogenic ancestor, as discussed above. In Clade B, CLEs of *Haemaphysalis*  
23  
24  
25 146 ticks are present along with a presumably pathogenic *Coxiella* that caused horse  
26  
27  
28 147 infection (Seo et al. 2016). Clade C has CRT, a pathogen-derived endosymbiont, along  
29  
30  
31 148 with strains that caused opportunistic human skin infections (Gottlieb et al. 2015;  
32  
33  
34 149 Angelakis et al. 2016; Guimard et al. 2017; Tsementzi et al. 2018; Ben-Yosef et al. 2020).  
35  
36 150 Only Clade D, which contains small-genomed CLEs (e.g., CLEAA), has no known  
37  
38  
39 151 pathogenic representatives. This phylogenetic pattern of endosymbionts clustering with  
40  
41  
42 152 pathogens indicate that, similar to the pathogenic ancestry of CLEOA and CRT, CLEs of  
43  
44  
45 153 several other ticks have also evolved from pathogenic coxiellae. Thus, based on  
46  
47  
48 154 phylogenetic and T4BSS distribution patterns, we surmise that *Coxiella* strains that  
49  
50  
51 155 infect vertebrates (e.g., humans, horses, birds) and invertebrates (e.g., crayfish) are  
52  
53  
54 156 widespread across the globe (**Fig. 3**), and many of them have evolved into tick  
55  
56  
57 157 endosymbionts.  
58  
59  
60

158

**HGT was a major contributor to gene accumulation in *C. burnetii*'s ancestors**

In order to better understand the evolution of *C. burnetii*, we traced the ancestry of its protein-coding genes by determining whether their orthologs — either functional or pseudogenized — were present in other Legionellales members. Out of 1,530 protein-coding genes whose ancestries we could trace, 790 were deemed to be ancestral, meaning it was present in the ancestor that diverged from *Legionella* (Node 1), and an additional 585 genes originated in Nodes 2-4 (Fig. 4; Supplemental Table S4). This data demonstrates that the common ancestor of *C. burnetii* and CLEOA contained most of the genes, including virulence factors, present in *C. burnetii*, and was hence well equipped to infect mammals.

A major impediment to unspooling the evolutionary history of *C. burnetii* is the sparse availability of Coxiellaceae genomes, which makes it difficult to ascertain whether genes were gained by *C. burnetii*'s ancestors at a Nodes 2-5 or were instead lost in other bacteria represented at each node. To overcome this difficulty, we calculated each *C. burnetii* gene's nucleotide composition (%GC) and Codon Adaptation Index (CAI), two measures known to distinguish foreign-origin genes from ancestral ones (Fig. 4; Supplemental Table S5; Sharp and Li 1987; Lawrence and Ochman 1997; Jansen et al. 2003; Raghavan et al. 2012). Both %GC and CAI values for genes that originated in Nodes 3-5 were significantly different from those of ancestral (Node 1) genes, indicating

1  
2  
3 178 that a considerable portion of these genes were likely acquired horizontally. [Node 2  
4  
5  
6 179 genes were excluded from this analysis due to small sample size ( $n=13$ ).] Interestingly,  
7  
8  
9 180 %GC and CAI values for Node 5 genes were not significantly different from those  
10  
11  
12 181 gained at Node 4, suggesting that many of the genes currently found only in the human  
13  
14 182 pathogen were present in the common ancestor of *C. burnetii* and CLEOA, and were  
15  
16  
17 183 later lost in the tick endosymbiont. However, it is clear that HGT has contributed to the  
18  
19  
20 184 accumulation of genes at Node 5 as well because 88 out of 155 genes in this category  
21  
22 185 showed phylogenetic patterns consistent with HGT (Supplemental Fig. S1, Table S6).  
23  
24  
25 186 Cumulatively, our results validate the important role HGT has played in assembling *C.*  
26  
27  
28 187 *burnetii*'s protein repertoire (Moses et al. 2017), and show that this process occurred  
29  
30  
31 188 principally in ancestors that preceded the *C. burnetii*-CLEOA split.  
32

### 33 189

### 34

### 35

### 36 190 **CLEOA potentially provides *O. amblus* with nutrients missing in vertebrate blood**

### 37

38 191 Similar to other hematophagic organisms (Duron and Gottlieb 2020), ticks likely obtain  
39  
40  
41 192 nutrients missing in blood from endosymbiotic bacteria such as CLEs and FLEs  
42  
43  
44 193 (Gottlieb et al. 2015; Smith et al. 2015; Gerhart et al. 2016, 2018; Duron et al. 2018;  
45  
46  
47 194 Tsementzi et al. 2018). In accordance with this idea, although CLEOA has lost a large  
48  
49  
50 195 number of genes (**Table 1**), it has retained complete pathways for the synthesis of  
51  
52  
53 196 several B-vitamins and cofactors (**Fig. 5**). Interestingly, these pathways are also present  
54  
55  
56 197 in *C. burnetii*, indicating that the genes are of ancestral origin and could be critical to the  
57  
58  
59  
60

1  
2  
3 198 intracellular growth of both the endosymbiont and the human pathogen.  
4

5  
6 199 CLEOA also contains 91 genes that are absent or have been deactivated in *C.*  
7

8  
9 200 *burnetii* (Supplemental Table S7). It is likely that many of these CLEOA-specific genes  
10

11  
12 201 have functions in the tick ecosystem but are not useful during mammalian infections.  
13

14 202 Collectively, based on its genomic features (**Table 1**), recent loss of T4BSS (**Fig. 2**), and  
15

16  
17 203 presence of intact pathways for synthesizing B vitamins and cofactors (**Fig. 5**), we  
18

19  
20 204 conclude that a pathogenic *Coxiella* was recruited to function as a nutrient-provisioning  
21

22  
23 205 endosymbiont in *O. amblus*.  
24

25 206  
26

27  
28 207  
29

30 208 **CLEOA has not retained genes that allow *C. burnetii* to withstand the harsh environs**  
31

32  
33 209 **of CCV**  
34

35  
36 210 **Loss of T4BSS and associated genes.** Because *C. burnetii* diverged from CLEOA  
37

38  
39 211 recently, it provided us an opportunity to perform a thorough comparison of the  
40

41  
42 212 human pathogen's genome to that of a closely-related non-pathogen. Our analysis  
43

44  
45 213 identified 980 functional genes in *C. burnetii* whose orthologs have been either  
46

47  
48 214 pseudogenized or deleted in CLEOA (Supplemental Table S8). Among them are genes  
49

50  
51 215 for T4BSS and for effectors secreted through T4BSS (**Fig. 2**; Supplemental Table S2) that  
52

53  
54 216 enable *C. burnetii* to generate its intracellular replicative niche, termed *Coxiella*-  
55

56  
57 217 containing vacuole (CCV) (Chen et al. 2010; Beare et al. 2011; Martinez et al. 2014, 2020;  
58  
59  
60

1  
2  
3 218 Newton et al. 2014). In addition, genes for PmrAB and EirA that control T4BSS activity,  
4  
5  
6 219 and for eight T4BSS effectors present on *C. burnetii*'s QpH1 plasmid have been  
7  
8  
9 220 inactivated in CLEOA (Maturana et al. 2013; Beare et al. 2014; Kuba et al. 2020).

10  
11 221 Therefore, the secretion system, which is critical to the intra-macrophage growth of *C.*  
12  
13  
14 222 *burnetii*, is clearly not required for CLEOA to grow within tick cells.  
15  
16

17 223

18  
19 224 **Loss of transporters of antibacterial molecules.** To protect itself from noxious  
20  
21  
22 225 molecules produced by the host, *C. burnetii* likely depends on transport proteins that  
23  
24  
25 226 efflux harmful substances out of its cytoplasm. For instance, macrophages increase  $\text{Cu}^{2+}$   
26  
27  
28 227 concentration within phagosomes to kill intracellular bacteria (Neyrolles et al. 2015),  
29  
30  
31 228 and *C. burnetii* probably utilizes a P-1B type ATPase to export copper from its  
32  
33  
34 229 cytoplasm to sustain intracellular growth (Rowland and Niederweis 2012). This  
35  
36  
37 230 ATPase, along with 18 others of unknown function, have been pseudogenized or  
38  
39  
40  
41 231 deleted in CLEOA (Supplemental Table S9). In addition, *C. burnetii* encodes 25 putative  
42  
43  
44 232 transporters that could facilitate the pathogen's growth within CCV, out of which, 19  
45  
46  
47 233 have become non-functional in CLEOA (Supplemental Table S9), suggestive of the mild  
48  
49  
50 234 nature of the tick endosymbiont's intracellular compartment where antibacterial  
51  
52  
53 235 molecules are probably not a major threat.  
54  
55  
56  
57  
58  
59  
60 236

1  
2  
3 237 **Diminished pH regulation.** A defining feature of CCV is its acidity (pH ~4.75) (Vallejo  
4  
5  
6 238 Esquerra et al. 2017; Samanta et al. 2019). To compensate, *C. burnetii* utilizes several  
7  
8  
9 239 mechanisms to maintain its cytoplasmic pH close to neutral (Hackstadt 1983), many of  
10  
11  
12 240 which have been rendered non-functional in CLEOA. For example, the enzyme  
13  
14 241 carbonic anhydrase that catalyzes the production of bicarbonate ( $\text{HCO}_3^-$ ) buffer from  
15  
16  
17 242  $\text{CO}_2$  (Vallejo Esquerra et al. 2017; Bury-Moné et al. 2008) has been pseudogenized in  
18  
19  
20 243 CLEOA (Supplemental Table S10). Another pH-regulating strategy used by *C. burnetii* is  
21  
22  
23 244 to remove excess protons in its cytoplasm via proton-antiporters such as the multi-  
24  
25 245 protein Mrp antiporter, a pair of  $\text{Na}^+/\text{H}^+$  antiporters, and a  $\text{K}^+/\text{H}^+$  antiporter. *C. burnetii*  
26  
27  
28 246 also encodes a pair of glutamate/gamma-aminobutyrate (GABA) antiporters that export  
29  
30  
31 247 GABA in exchange for glutamate, thereby reducing the cytoplasmic proton content. The  
32  
33  
34 248 Mrp antiporter, one of the two  $\text{Na}^+/\text{H}^+$  antiporters, and both glutamate/GABA  
35  
36 249 antiporters have been pseudogenized in CLEOA (Supplemental Table S10). A hallmark  
37  
38  
39 250 of *C. burnetii* is its unusually high number of basic proteins (~46% of proteins have pI  
40  
41  
42 251 values  $\geq 9$ ; average pI 8.22) that could function as a “proton sink,” which allows the  
43  
44  
45 252 pathogen to maintain its cytoplasmic pH close to neutral (Seshadri et al. 2003). In  
46  
47  
48 253 contrast, only ~39% of proteins in CLEOA have pI values  $\geq 9$  (average pI 8.0), again  
49  
50  
51 254 illustrating a lack of acidic stress within CLEOA’s intracellular vacuole. Collectively,  
52  
53  
54 255 our data suggest that the endosymbiont does not face the constant threat of excess  
55  
56  
57  
58  
59  
60

1  
2  
3 256 protons entering its cytoplasm, probably because its intracellular niche, unlike *C.*  
4  
5  
6 257 *burnetii*'s, has a pH closer to neutral.  
7

8  
9 258

10  
11 259 **Loss of cell membrane and cell wall genes.** In gram-negative bacteria, inner and outer  
12  
13  
14 260 membranes along with peptidoglycan play important roles in stress response (Rowlett  
15  
16  
17 261 et al. 2017). In CLEOA, the gene that encodes PlsC, which converts lysophosphatidic  
18  
19  
20 262 acid into phosphatidic acid (PA), a universal intermediate in the biosynthesis of  
21  
22  
23 263 membrane phospholipids, has been pseudogenized. The *plsC* gene is essential in  
24  
25 264 *Escherichia coli*, and a transposon insertion in this gene in *C. burnetii* caused severe  
26  
27  
28 265 intracellular growth defect (Coleman 1990; Martinez et al. 2014); hence, it is not clear  
29  
30  
31 266 how CLEOA is able to build its membranes without a functional *plsC*, but one  
32  
33  
34 267 possibility is that the endosymbiont utilizes PA obtained from its host. Another  
35  
36 268 membrane-associated loss of function in CLEOA is the pseudogenization of the *pldA*  
37  
38  
39 269 gene that encodes phospholipase A (PldA), which is critical to *C. burnetii*'s outer  
40  
41  
42 270 membrane function and for optimal growth within macrophages (Stead et al. 2018). As  
43  
44  
45 271 for its peptidoglycan, CLEOA contains intact genes for D, D-transpeptidases (also  
46  
47  
48 272 known as penicillin-binding proteins) that catalyze 4-3 peptide cross-links between D-  
49  
50  
51 273 alanine and diaminopimelate; however, all L, D-transpeptidase genes (annotated as  
52  
53  
54 274 "enhanced entry proteins") have been pseudogenized, indicating that the tick symbiont  
55  
56  
57 275 does not have the ability to generate 3-3 cross-links between diaminopimelate  
58  
59  
60



1  
2  
3 276 molecules in its peptidoglycan. These nonclassical cross-links contribute to *C. burnetii*'s  
4  
5  
6 277 environmental stability (Sandoz et al. 2016), and are probably not critical to CLEOA  
7  
8  
9 278 because the endosymbiont is passed vertically from one generation to next. Collectively,  
10  
11  
12 279 as observed in other endosymbionts (Nakabachi et al. 2006; McCutcheon and Moran  
13  
14 280 2010; Chong and Moran 2018), CLEOA lacks numerous proteins that are typically  
15  
16  
17 281 considered integral to the optimal functioning of bacterial cell membrane and cell wall.  
18

19 282  
20  
21  
22 283 **Loss of antioxidant genes.** An intricate network of antioxidants allows *C. burnetii* to  
23  
24 284 thrives in a phagolysosome-derived intracellular vacuole (Mertens and Samuel 2012). In  
25  
26  
27 285 contrast to CCV, oxidative stress appears to be minimal in CLEOA's intracellular  
28  
29  
30 286 vacuole because the endosymbiont contains only a streamlined version of *C. burnetii*'s  
31  
32  
33 287 antioxidant defense system. For instance, *C. burnetii* contains two superoxide  
34  
35  
36 288 dismutases (SODs), but CLEOA has retained the cytoplasmic Fe-containing SodB, but  
37  
38  
39 289 not SodC, the periplasmic Cu/Zn-SOD. OxyR, the master regulator of peroxide stress,  
40  
41  
42 290 along with a catalase, a peroxidase (AhpC2), a methionine sulfoxide reductase, a  
43  
44  
45 291 hemerythrin-like protein, and a glutathione transferase that together help mitigate  
46  
47  
48 292 oxidative stress have also been deactivated in CLEOA (Supplemental Table S11). In  
49  
50  
51 293 addition, *C. burnetii*, but not CLEOA, has the ability to synthesize queuine, a guanine  
52  
53  
54 294 analog, found in the first anticodon position of several post-transcriptionally modified  
55  
56  
57 295 tRNAs (Iwata-Reuyl 2003). The precise functions of queuine is not understood, but it is

1  
2  
3 296 thought to promote the activity of antioxidant enzymes, including catalase, superoxide  
4  
5  
6 297 dismutase, and glutathione transferase, most of which, as mentioned above, have lost  
7  
8  
9 298 their functionality in CLEOA (Koh and Sarin 2018).

10  
11 299 *C. burnetii* utilizes both cytochrome bd (encoded by genes *cydABX*) and  
12  
13  
14 300 cytochrome o (encoded by genes *cyoABCD*) as terminal oxidases, but CLEOA has only  
15  
16  
17 301 retained cytochrome o genes. Cytochrome bd, which also functions as a quinol  
18  
19  
20 302 peroxidase that prevents the buildup of oxidative free radicals (Endley et al. 2001;  
21  
22  
23 303 Omsland and Heinzen 2011), has become nonfunctional in the tick endosymbiont. In  
24  
25  
26 304 addition, CLEOA does not encode genes for an acid phosphatase and two sterol  
27  
28  
29 305 reductases that likely modify host proteins and cholesterol, respectively, to protect *C.*  
30  
31  
32 306 *burnetii* from host-induced oxidative stress (Seshadri et al. 2003; Gilk et al. 2010; Hill and  
33  
34  
35 307 Samuel 2011; Gilk 2012). Finally, *C. burnetii* is thought to compensate for the lack of the  
36  
37  
38 308 oxidative branch of Pentose Phosphate Pathway (PPP)— a major source of NADPH, by  
39  
40  
41 309 utilizing alternative NADPH-regenerating enzymes such as short chain  
42  
43  
44 310 dehydrogenases and sterol reductases, and by salvaging NAD<sup>+</sup> from the host (Bitew et  
45  
46  
47 311 al. 2018, 2020). In CLEOA, all four short chain dehydrogenases, the two eukaryote-like  
48  
49  
50 312 sterol reductases, and the nicotinate-salvaging protein have become nonfunctional. In  
51  
52  
53 313 total, while the human pathogen contains several mechanisms to defend against  
54  
55  
56 314 oxidative stress, most of these antioxidant systems have been lost in CLEOA, most  
57  
58  
59 315 likely due to minimal oxidative stress experienced by the bacterium within tick cells.  
60

1  
2  
3 316 Collectively, the loss of T4BSS, transporters, pH regulation, cell wall modification, and  
4  
5  
6 317 antioxidant defense in CLEOA show that its intracellular vacuole is a less stressful place  
7  
8  
9 318 to live than the phagolysosome-derived CCV occupied by *C. burnetii*.

10  
11 319

### 14 320 **Heme analog inhibits *C. burnetii* growth**

16  
17 321 Cytochromes require heme as a cofactor, but CLEOA does not contain a functional  
18  
19 322 heme biosynthesis pathway, which is present in *C. burnetii* (Supplemental Table S12).  
20  
21  
22 323 The only intact heme biosynthesis gene in CLEOA is *ctaB*, which encodes an enzyme  
23  
24  
25 324 that converts heme b to heme o, a component of cytochrome o — the sole terminal  
26  
27  
28 325 cytochrome oxidase present in CLEOA (Saiki et al. 1992). Based on this evidence, the  
29  
30  
31 326 endosymbiont appears to import heme b from the tick hemocoel (vertebrate  
32  
33 327 hemoglobin contains heme b) and converts it to heme o using the *ctaB*-encoded  
34  
35  
36 328 protoheme IX farnesyltransferase. Additionally, while *C. burnetii* can import ferrous  
37  
38  
39 329 iron released from iron-containing host molecules such as ferritin and transferrin  
40  
41  
42 330 (Sanchez and Omsland 2020), free Fe<sup>2+</sup> does not seem to be important for CLEOA's  
43  
44  
45 331 intracellular growth because the iron transporter FeoB has been pseudogenized,  
46  
47  
48 332 suggesting that host-derived heme b serves as the tick endosymbiont's heme and iron  
49  
50  
51 333 source.

52 334 The heme biosynthesis pathway, while absent in CLEOA, is conserved in all  
53  
54  
55 335 strains of *C. burnetii*, probably because the iron-protoporphyrin molecule is critical to

1  
2  
3 336 the pathogen's ability to grow within human macrophages (Moses et al. 2017). We  
4  
5  
6 337 tested *C. burnetii*'s dependence on heme by treating both axenically grown and  
7  
8  
9 338 intracellular *C. burnetii* with gallium protoporphyrin IX (GaPPIX), which can replace  
10  
11  
12 339 heme in cytochromes and other heme-containing enzymes (Hijazi et al. 2017, 2018). As  
13  
14 340 shown in **Fig. 6**,  $\geq 250$  nM of GaPPIX caused significant inhibition of *C. burnetii* growth  
15  
16  
17 341 in ACCM-2, and treatment with  $\geq 2$   $\mu$ M of GaPPIX resulted in significant growth  
18  
19  
20 342 impairment of *C. burnetii* within THP-1 cells. Reassuringly, only GaPPIX concentrations  
21  
22  
23 343 of  $\geq 512$   $\mu$ M caused cytotoxicity in THP-1 cells (Fig. 6C), indicating that gallium  
24  
25  
26 344 compounds could potentially be used to treat *C. burnetii* infections.  
27  
28  
29

345

## 30 346 **DISCUSSION**

31  
32  
33 347 Although symbiotic and pathogenic coxiellae associated with ticks are found across the  
34  
35  
36 348 globe, it is not clear how pathogenesis and symbiosis evolved in this group of bacteria.  
37  
38  
39 349 Here we show that CLEOA, a soft-tick symbiont, and *C. burnetii*, a human pathogen,  
40  
41  
42 350 evolved recently from a common ancestor that contained genes necessary to infect  
43  
44  
45 351 macrophages. Additionally, while HGT contributed significantly to the evolution of *C.*  
46  
47  
48 352 *burnetii*, it occurred in ancestors prior to the divergence of CLEOA and *C. burnetii*  
49  
50  
51 353 lineages. These discoveries clarify the evolution of *C. burnetii*, which previously was  
52  
53  
54 354 thought to have evolved from an avirulent tick endosymbiont by gaining virulence  
55  
56  
57 355 factors via HGT. We further show that the evolution of *C. burnetii* and CLEOA fits into a  
58  
59  
60

1  
2  
3 356 general pattern of tick-associated coxiellae originating from pathogens, thereby  
4  
5  
6 357 revealing that CLEs, as described previously for FLEs, originated from pathogenic  
7  
8  
9 358 ancestors. Lastly, by comparing the genomes of *C. burnetii* and CLEOA, we were able to  
10  
11  
12 359 gain new insights into the intracellular biology of both bacteria, and show that  
13  
14 360 metabolic pathways retained only in the human pathogen are promising targets for the  
15  
16  
17 361 development of new treatments against Q fever.

18  
19  
20 362 **Emergence of tick-symbionts from virulent ancestors.** *Coxiella* species related to CLEs  
21  
22  
23 363 infect a wide range of animals (Shivaprasad et al. 2008; Woc-Colburn et al. 2008;  
24  
25  
26 364 Angelakis et al. 2016; Seo et al. 2016; Guimard et al. 2017; Elliman and Owens 2020;  
27  
28  
29 365 Needle et al. 2020), but these infectious strains are not the closest relatives of *C. burnetii*;  
30  
31  
32 366 instead, the human pathogen's closest relative is the soft-tick symbiont CLEOA. Akin to  
33  
34  
35 367 the CLEOA-*C. burnetii* relationship, CRT, the endosymbiont in *R. turanicus*, is closely  
36  
37 368 related to pathogenic *Coxiella* (termed "*Candidatus* *Coxiella massiliensis*") isolated from  
38  
39  
40 369 human skin infections, and a strain of *Coxiella* isolated from horse blood is closely  
41  
42  
43 370 related to CLEs present in *Haemaphysalis* ticks (Angelakis et al. 2016; Seo et al. 2016;  
44  
45  
46 371 Guimard et al. 2017). In addition to these pathogens, bacteria related to CLEs have  
47  
48  
49 372 repeatedly caused fatal bird and crayfish infections (**Fig. 3**; Shivaprasad et al. 2008;  
50  
51  
52 373 Woc-Colburn et al. 2008; Elliman and Owens 2020; Needle et al. 2020). Microscopic and  
53  
54  
55 374 histological data from avian infections demonstrated that the bacteria have the ability to  
56  
57  
58 375 generate CCV-like compartments within macrophages, and both avian and human skin  
59  
60

1  
2  
3 376 infection strains have “small-cell” and “large-cell” morphologies — two distinct  
4  
5  
6 377 characteristics of *C. burnetii* — suggesting that the bacteria are genuine vertebrate  
7  
8  
9 378 pathogens (Shivaprasad et al. 2008; Woc-Colburn et al. 2008; Angelakis et al. 2016;  
10  
11 379 Guimard et al. 2017; Needle et al. 2020). Further research, including sequencing their  
12  
13  
14 380 genomes, is required to elucidate the biology and pathogenicity of these infective  
15  
16  
17 381 strains and to understand why only one, i.e., *C. burnetii*, among several virulent lineages  
18  
19  
20 382 have evolved into a bona fide human pathogen.

21  
22  
23 383 **Tick endosymbionts are ephemeral.** Phylogenies of only a few CLEs are congruent  
24  
25  
26 384 with those of their hosts (Duron et al. 2017; Binetruy et al. 2020), probably because older  
27  
28  
29 385 CLEs get replaced by newer CLEs derived from distantly-related coxiellae. In a similar  
30  
31  
32 386 fashion, FLEs seem to have replaced older CLEs in several tick lineages (Gerhart et al.  
33  
34 387 2016, 2018; Duron et al. 2017, 2018). This ephemeral nature of CLEs is surprising  
35  
36  
37 388 because hematophagous arthropods typically need a reliable partner to gain nutrients  
38  
39  
40 389 that are in short supply in vertebrate blood (Duron and Gottlieb 2020; Duarte et al. 1999;  
41  
42 390 Sterkel et al. 2017). Insects such as bedbugs and body lice that face similar nutrient  
43  
44  
45 391 scarcity have evolved stable long-term relationships with endosymbionts (Perotti et al.  
46  
47  
48 392 2007; Hosokawa et al. 2010). It is not clear why that is not the case in ticks, but one  
49  
50  
51 393 possibility is that ticks do not need to establish long-term relationships because they  
52  
53  
54 394 frequently encounter pathogenic bacteria that are predisposed to becoming nutrient-  
55  
56 395 provisioning endosymbionts. Another reason for the unstable nature of CLE-tick

1  
2  
3 396 relationships could be that the constant turnover of endosymbionts protects ticks from  
4  
5  
6 397 being dependent on an endosymbiont with reduced nutrient-provisioning capability  
7  
8  
9 398 (Russell et al. 2017; Bennett and Moran 2020). Gaining new symbionts via horizontal  
10  
11  
12 399 transmission could also protect ticks from becoming dependent on a degraded  
13  
14 400 endosymbiont. While the mechanistic details of this process are not understood,  
15  
16  
17 401 phylogenetic patterns of CLE and FLE distribution strongly indicate the occurrence of  
18  
19  
20 402 horizontal transmission of bacteria between ticks (Gerhart et al. 2016, 2018; Duron et al.  
21  
22  
23 403 2017; Binetruy et al. 2020). It should be noted however that not all tick-endosymbionts  
24  
25 404 are short-lived. Ticks that carry CLEs belonging to Clade D (**Fig. 3**) appear to have  
26  
27  
28 405 established long-term relationships with their endosymbionts. For instance, CLEs in *A.*  
29  
30 406 *americanum* and *A. sculptum* have highly reduced (~0.60 Mbp) genomes that are similar  
31  
32  
33 407 in size to *Buchnera*, which established its symbiosis with aphids more than 200 million  
34  
35  
36 408 years ago (Moran et al. 1993). Putting all this information together, it appears that a  
37  
38  
39 409 combination of vertical inheritance, horizontal transmission, and periodic replacement  
40  
41  
42 410 of old symbionts with new pathogen-derived symbionts underlies the complex  
43  
44  
45 411 distribution pattern of endosymbionts observed in ticks (Gottlieb et al. 2015; Smith et al.  
46  
47  
48 412 2015; Gerhart et al. 2016, 2018; Duron et al. 2017; Tsementzi et al. 2018; Binetruy et al.  
49  
50 413 2020).

51  
52 414  
53  
54  
55  
56  
57  
58  
59  
60

1  
2  
3 415 **Functions of CLEs and FLEs.** While the exact functions of FLEs and CLEs have not been  
4  
5  
6 416 fully characterized, previous studies have shown that they infect tick ovaries and are  
7  
8  
9 417 often the predominant bacterium present in long-term laboratory tick colonies, an  
10  
11  
12 418 indication that the bacteria are vertically transmitted and are essential to ticks'  
13  
14 419 wellbeing (Reinhardt et al. 1972; Klyachko et al. 2007; Buysse et al. 2019; Smith et al.  
15  
16  
17 420 2015; Gerhart et al. 2016, 2018). In addition, removal of the resident endosymbiont via  
18  
19  
20 421 antibiotic treatment reduced tick fitness, which was reversed when ticks were provided  
21  
22  
23 422 with B vitamins (Zhong et al. 2007; Smith et al. 2015; Gerhart et al. 2016; Guizzo et al.  
24  
25  
26 423 2017; Zhang et al. 2017; Duron et al. 2018; Li et al. 2018; Ben-Yosef et al. 2020). Our  
27  
28  
29 424 genome analyses support a nutrient-provisioning role for tick endosymbionts because  
30  
31  
32 425 the genes required to synthesize several B vitamins and cofactors are conserved in all  
33  
34  
35 426 CLEs and FLEs. Future experiments should clarify whether any or all of these nutrients  
36  
37  
38 427 form the basis for the CLE-tick and FLE-tick symbioses.  
39  
40

41 429 **Pathogen-specific metabolic processes are potential targets to control Q fever.** Genetic  
42  
43  
44 430 and physiological capabilities accumulated by a bacterium are critical to its ability to  
45  
46  
47 431 adapt to new environments, especially ones such as intra-macrophage vacuoles that do  
48  
49  
50 432 not facilitate the gain of new genes via HGT. In accordance with this idea, our analyses  
51  
52  
53 433 showed that virulence factors and metabolic genes utilized by *C. burnetii* to grow within  
54  
55  
56 434 CCV were present in the common ancestor of *C. burnetii* and CLEOA. Befitting its



1  
2  
3 435 obligate endosymbiotic lifestyle, many of these genes have become non-functional in  
4  
5  
6 436 CLEOA, allowing us to identify metabolic processes that are likely critical to *C.*  
7  
8  
9 437 *burnetii*'s intracellular growth. One metabolite that is exclusively produced by the  
10  
11  
12 438 pathogen is heme, the iron-protoporphyrin required for oxidative phosphorylation,  
13  
14 439 among other functions. To test the importance of heme to *C. burnetii*, we exposed the  
15  
16  
17 440 bacterium to GaPPIX, a Ga(III) complex of protoporphyrin IX. Ga(III) inhibits bacterial  
18  
19  
20 441 growth because it binds to biological complexes that normally binds to Fe(III), but  
21  
22 442 under physiological conditions Ga(III) is not reduced to Ga(II), thereby disrupting  
23  
24  
25 443 essential redox-driven biological processes (Bernstein 1998). We chose GaPPIX over  
26  
27  
28 444 other gallium-based formulations because it could replace heme in cytochromes, is  
29  
30  
31 445 known to be bactericidal, and is not toxic to primary human fibroblasts and established  
32  
33  
34 446 cell lines (Stojiljkovic et al. 1999; Arivett et al. 2015; Hijazi et al. 2018). *C. burnetii* lacks  
35  
36  
37 447 homologs of known heme transporters (Moses et al. 2017), hence, it is not clear how  
38  
39  
40 448 GaPPIX enters into the pathogen, but our growth assays clearly demonstrated that the  
41  
42  
43 449 heme analog is very effective at inhibiting both axenic and intracellular growth of *C.*  
44  
45  
46 450 *burnetii* (Fig. 6). Encouragingly, a recent human trial showed that Ga could improve  
47  
48  
49 451 lung function in people with cystic fibrosis and chronic *Pseudomonas aeruginosa* lung  
50  
51  
52 452 infections, and that the molecule worked synergistically with other antibiotics to inhibit  
53  
54  
55 453 bacterial growth (Goss et al. 2018). Although further work is required to gauge its  
56  
57  
58 454 impact on human microbiome, Ga, which has been approved by FDA for intravenous  
59  
60

1  
2  
3 455 administration (Bonchi et al. 2014), and its derivatives such as GaPPIX, hold great  
4  
5  
6 456 promise as new therapeutic tools.  
7  
8  
9

10 457

## 11 458 **METHODS**

12  
13  
14  
15 459 **Genome sequencing and assembly.** An *O. amblus* female, collected from soil  
16  
17  
18 460 underneath rocks near a *Spheniscus humboldti* (Humboldt penguin) nesting area in Isla  
19  
20  
21 461 Grande de Atacama, Chile, was identified as described in Clifford *et al.* 1980. DNA was  
22  
23 462 extracted from the tick using DNeasy Blood & Tissue kit (Qiagen) and was submitted to  
24  
25  
26 463 Yale Center for Genome Analysis for Illumina (NovaSeq) sequencing. The resulting 150  
27  
28  
29 464 bp paired-end reads were trimmed using Trimmomatic resulting in approximately 220  
30  
31  
32 465 million read pairs of suitable quality (Bolger et al. 2014). The reads were assembled into  
33  
34 466 contigs using metaSPAdes (Nurk et al. 2017), and open reading frames (ORFs) were  
35  
36  
37 467 identified using Prodigal (Hyatt et al. 2010). RNAMmer (Lagesen et al. 2007) was used to  
38  
39  
40 468 identify ribosomal RNA in all contigs and sequencing coverage values were used to  
41  
42  
43 469 determine the relative abundance of bacteria: 88.5% *Coxiella*, 4.6% *Alkalihalobacillus*, 3.8%  
44  
45 470 *Sporosarcina*, and 3.1% *Oceanobacillus*.

46  
47  
48 471 Contigs containing *Coxiella* genes were tentatively identified using BLASTn and  
49  
50  
51 472 BLASTp by comparing to a database of all publicly available sequences from  
52  
53 473 Coxiellacea members. CONCOCT (Alneberg et al. 2014) was used for binning contigs  
54  
55  
56 474 based on coverage and k-mer composition, and these findings were merged with  
57  
58  
59  
60

1  
2  
3 475 BLAST-based binning results. Approximately 20 million paired reads that mapped to  
4  
5  
6 476 contigs identified as containing *Coxiella* genes were used for a final metaSPAdes  
7  
8  
9 477 assembly resulting in a total of 101 contigs. The final collection of contigs was verified  
10  
11  
12 478 using hmmsearch (Potter et al. 2018) to identify essential single-copy genes (Albertsen  
13  
14 479 et al. 2013), as well as RNAmmer (Lagesen et al. 2007) and tRNAscan-SE (Chan and  
15  
16  
17 480 Lowe 2019) to identify ribosomal and transfer RNAs, respectively. We were unable to  
18  
19  
20 481 stitch the contigs together into a closed chromosome because 49 out of the 101 CLEOA  
21  
22  
23 482 contigs contained the insertion sequence IS1111 at one or both ends. Similar to the  
24  
25  
26 483 CLEOA genome, multiple copies of IS1111 is present in the genomes of other CLEs and  
27  
28  
29 484 *C. burnetii*, and is known to have an impact on genome evolution and gene content  
30  
31  
32 485 (Duron 2015; Beare et al. 2009). Although we couldn't close the genome, the presence of  
33  
34  
35 486 106 out of 111 highly conserved single-copy genes in both CLEOA and *C. burnetii*  
36  
37  
38 487 indicate that most of the CLEOA genome is represented in the assembled contigs. The  
39  
40  
41 488 final set of 101 contigs were submitted to NCBI (accession VFIV00000000) and  
42  
43  
44 489 annotated using the Prokaryotic Genome Pipeline.

45  
46  
47 491 **Phylogenetic analysis.** Orthofinder (Emms and Kelly 2015) was utilized to identify 205  
48  
49  
50 492 single-copy genes present in 52 representative species from the order Legionellales  
51  
52  
53 493 (Supplemental Tables S1, S13) in order to build the comprehensive phylogenomic tree  
54  
55  
56 494 Supplemental Fig. S2. A subset of 117 genes conserved in 30 species (Supplemental

1  
2  
3 495 Tables S1, S13) were used to generate **Fig. 1**. For both trees, nucleotide sequences were  
4  
5  
6 496 aligned individually using global MAFFT (Kato and Standley 2013) and were then  
7  
8  
9 497 concatenated. GBlocks (Talavera and Castresana 2007) was used to cull ambiguously  
10  
11  
12 498 aligned regions and jModelTest2 (Darriba et al. 2012) was used to select the appropriate  
13  
14 499 model (GTR+I+G). Maximum Likelihood trees were generated using RaxML and  
15  
16  
17 500 Bayesian trees were produced using MrBayes (Ronquist et al. 2012; Stamatakis 2014).  
18  
19  
20 501 The 16S rDNA trees were built using the same process as above, with the final tree  
21  
22 502 based on 1203 nucleotide positions, and nodes with less than 70% support collapsed. To  
23  
24  
25 503 confirm the HGT origin of Node 5 genes, homologs were identified via BLASTp (NCBI  
26  
27  
28 504 nr database, e-value  $\leq 10e-5$ , identity  $\geq 30\%$  identity, coverage  $\geq 70\%$ ). The nucleotide  
29  
30  
31 505 sequences of the homologs were collected into a database, and the Phylomizer pipeline  
32  
33 506 (<https://github.com/Gabaldonlab/phylomizer>) was used to generate individual  
34  
35  
36 507 Maximum Likelihood trees using the 75 most closely related homolog sequences. Each  
37  
38  
39 508 tree was then compared to an NCBI Taxonomy-based tree to validate HGT  
40  
41 509 (Supplemental Fig. S1).

42  
43  
44 510

45  
46 511 **Determination of nodes of gene origin.** The presence of functional homologs of *C.*  
47  
48  
49 512 *burnetii* RSA493 (AE016828.3) genes in other members of the order Legionellales was  
50  
51  
52 513 determined using BLASTp (identity  $\geq 30\%$ , coverage  $\geq 70\%$ , e-value  $\leq 10e-5$ ), and  
53  
54  
55 514 pseudogenized homologs were detected using tBLASTn (identity  $\geq 30\%$ , coverage  $\geq 50\%$ ,

1  
2  
3 515 e-value  $\leq 10e-5$ ). The presence/absence profile was utilized in Gain and Loss Mapping  
4  
5  
6 516 Engine (GLOOME) (Cohen et al. 2010) to determine the posterior probability of each  
7  
8  
9 517 gene's presence at nodes N1-N5. For each *C. burnetii* gene, the node of origin was  
10  
11  
12 518 marked as the oldest node at which posterior probability was  $\geq 0.7$ , with all subsequent  
13  
14 519 nodes also having posterior probability of  $\geq 0.7$ , as described previously (Peer and  
15  
16  
17 520 Margalit 2014). We also identified 409 genes that are conserved in all CLEs  
18  
19  
20 521 (Supplemental Table S14) using BLASTp (identity  $\geq 30\%$ , coverage  $\geq 70\%$ , e-value  $\leq 10e-$   
21  
22 522 5).

23  
24  
25 523  
26  
27  
28 524 **Calculation of CAI and pI.** We identified 22 highly conserved single-copy protein-  
29  
30  
31 525 coding genes in *C. burnetii* that were highly expressed in both ACCM-2 and within  
32  
33  
34 526 human macrophages based on previous RNA-seq data (Supplemental Table S5; Warri-  
35  
36  
37 527 et al. 2014; Wachter et al. 2019). CodonW (<http://codonw.sourceforge.net>) was used to  
38  
39  
40 528 generate CAI values for the 22 genes in order to generate a model for optimal codon  
41  
42  
43 529 usage in *C. burnetii*, which was then compared to CAI values of sets of genes acquired at  
44  
45  
46 530 each node. All 22 genes used to build the model belonged to Node 1, and were not  
47  
48  
49 531 included in this analysis. Potentially spurious genes (n=224) that did not have any  
50  
51  
52 532 detectable homologs outside of *C. burnetii*, as well as genes with undetermined nodes of  
53  
54  
55 533 origin (n=44) were excluded from this analysis (Supplemental Table S15). Isoelectric

1  
2  
3 534 points (pI) for all proteins in CLEOA and *C. burnetii* RSA493 (AE016828.3) were  
4  
5  
6 535 calculated using IPC (Kozlowski 2016).  
7  
8

9 536

### 11 537 **GaPPIX susceptibility assay**

12  
13  
14 538 A 10mM GaPPIX (Frontier Scientific) solution was prepared in dimethyl sulfoxide  
15  
16  
17 539 (DMSO) and was stored at 4°C under dark conditions until further use. *C. burnetii* was  
18  
19  
20 540 cultured in ACCM-2 for 2 days at 37°C, 5% CO<sub>2</sub> and 2.5% O<sub>2</sub>, and ~2x10<sup>7</sup> genome  
21  
22 541 equivalents were resuspended in fresh ACCM-2 containing 125nM, 250nM, 500nM,  
23  
24  
25 542 1mM, 2mM, 4mM, or 8mM GaPPIX in 96-well black-bottom microplates (Greiner Bio-  
26  
27  
28 543 One). Bacterial growth was measured using PicoGreen (Invitrogen) as described  
29  
30  
31 544 previously (Moses et al. 2017).  
32

33 545 THP-1 human monocytes (ATCC, TIB-202) were cultured in sterile RPMI-1640  
34  
35  
36 546 medium (Gibco) supplemented with 1mM sodium pyruvate, 0.05 mM beta-  
37  
38  
39 547 mercaptoethanol, 1% Pen-Strep, and 4500 mg/L glucose with 10% heat-inactivated fetal  
40  
41  
42 548 bovine serum (FBS) at 37°C, 5% CO<sub>2</sub> in 6-well tissue culture plates. Prior to infection,  
43  
44  
45 549 cells were differentiated into macrophages by treating with 30 nM phorbol 12-myristate  
46  
47  
48 550 13-acetate (PMA) for 24h, followed by resting in PMA-free RPMI for 24h. Infection of  
49  
50  
51 551 THP-1 cells with *C. burnetii* was carried out using a 7d bacterial culture at a multiplicity  
52  
53  
54 552 of infection of 25. After briefly washing the cells with PBS, bacteria-containing medium  
55  
56  
57 553 was added to each well and gently centrifuged for 10 minutes followed by incubation at  
58  
59  
60

1  
2  
3 554 37°C, 5% CO<sub>2</sub> for two hours. To remove extracellular bacteria, cells were washed three  
4  
5  
6 555 times with PBS, and replaced with antibiotic-free RPMI and were incubated for 48h  
7  
8  
9 556 before treating with GaPPIX- (2uM, 8uM, and 32uM) or DMSO- (as control) containing  
10  
11  
12 557 media. After 72h, cells were washed three times with PBS and intracellular bacterial  
13  
14 558 load was measure using qPCR, as we described previously (Moses et al. 2017). Potential  
15  
16  
17 559 cytotoxicity of GaPPIX was determined by measuring the levels of released lactate  
18  
19  
20 560 dehydrogenase (LDH) in cell supernatants using an LDH Cytotoxicity Assay Kit  
21  
22 561 (Invitrogen).

23  
24 56225  
26 56327  
28 56429  
30  
31  
32  
33 565 **DATA AVAILABILITY**

34  
35  
36 566 The CLEOA genome generated in this study has been submitted to the NCBI Assembly  
37  
38 567 database (<https://www.ncbi.nlm.nih.gov/assembly/>) under Whole Genome Shotgun  
39  
40 568 (WGS) accession prefix VFIV, BioSample SAMN12040594, and BioProject PRJNA548565.

41  
42 56943  
44  
45  
46 570 **ACKNOWLEDGEMENTS**

47  
48  
49 571 We thank Samantha Fancher, Andrew Ashford and Jim Archuleta for technical help,  
50  
51  
52 572 and Daniel González-Acuña for assisting in tick collection. This project was supported  
53  
54  
55 573 in part by NIH grants AI123464, AI126385, and AI133023 to R.R.

574

575

576

577 **REFERENCES**

- 578 Albertsen M, Hugenholtz P, Skarshewski A, Nielsen KL, Tyson GW, Nielsen PH. 2013.  
579 Genome sequences of rare, uncultured bacteria obtained by differential coverage  
580 binning of multiple metagenomes. *Nat Biotechnol* **31**: 533–538.
- 581 Almeida AP, Marcili A, Leite RC, Nieri-Bastos FA, Domingues LN, Martins JR, Labruna  
582 MB. 2012. *Coxiella* symbiont in the tick *Ornithodoros rostratus* (Acari: Argasidae).  
583 *Ticks Tick-Borne Dis* **3**: 203–206.
- 584 Alneberg J, Bjarnason BS, de Bruijn I, Schirmer M, Quick J, Ijaz UZ, Lahti L, Loman NJ,  
585 Andersson AF, Quince C. 2014. Binning metagenomic contigs by coverage and  
586 composition. *Nat Methods* **11**: 1144–1146.
- 587 Angelakis E, Mediannikov O, Jos S-L, Berenger J-M, Parola P, Raoult D. 2016. *Candidatus*  
588 *Coxiella massiliensis* infection. *Emerg Infect Dis* **22**: 285–288.
- 589 Arivett BA, Fiester SE, Ohneck EJ, Penwell WF, Kaufman CM, Relich RF, Actis LA.  
590 2015. Antimicrobial activity of gallium protoporphyrin IX against *Acinetobacter*  
591 *baumannii* strains displaying different antibiotic resistance phenotypes.  
592 *Antimicrob Agents Chemother* **59**: 7657–7665.
- 593 Beare PA, Gilk SD, Larson CL, Hill J, Stead CM, Omsland A, Cockrell DC, Howe D,  
594 Voth DE, Heinzen RA. 2011. Dot/Icm type IVB secretion system requirements for  
595 *Coxiella burnetii* growth in human macrophages. *mBio* **2**: e00175-00111.
- 596 Beare PA, Sandoz KM, Larson CL, Howe D, Kronmiller B, Heinzen RA. 2014. Essential  
597 role for the response regulator PmrA in *Coxiella burnetii* type 4B secretion and  
598 colonization of mammalian host cells. *J Bacteriol* **196**: 1925–1940.
- 599 Ben-Yosef M, Rot A, Mahagna M, Kapri E, Behar A, Gottlieb Y. 2020. *Coxiella*-like  
600 Endosymbiont of *Rhipicephalus sanguineus* is required for physiological processes  
601 during ontogeny. *Front Microbiol* **11**: 493.



- 1  
2  
3 602 Bennett GM, Moran NA. 2015. Heritable symbiosis: The advantages and perils of an  
4 603 evolutionary rabbit hole. *Proc Natl Acad Sci U S A* **112**: 10169–10176.  
5  
6  
7 604 Bernstein LR. 1998. Mechanisms of therapeutic activity for gallium. *Pharmacol Rev* **50**:  
8 605 665–682.  
9  
10  
11 606 Binetruy F, Buysse M, Lejarre Q, Barosi R, Villa M, Rahola N, Paupy C, Ayala D, Duron  
12 607 O. 2020. Microbial community structure reveals instability of nutritional  
13 608 symbiosis during the evolutionary radiation of *Amblyomma* ticks. *Mol Ecol* **29**:  
14 609 1016–1029.  
15  
16  
17 610 Bitew MA, Hofmann J, De Souza DP, Wawegama NK, Newton HJ, Sansom FM. 2020.  
18 611 SdrA, an NADP(H)-regenerating enzyme, is crucial for *Coxiella burnetii* to resist  
19 612 oxidative stress and replicate intracellularly. *Cell Microbiol* **22**: e13154.  
20  
21  
22 613 Bitew MA, Khoo CA, Neha N, De Souza DP, Tull D, Wawegama NK, Newton HJ,  
23 614 Sansom FM. 2018. De novo NAD synthesis is required for intracellular  
24 615 replication of *Coxiella burnetii*, the causative agent of the neglected zoonotic  
25 616 disease Q fever. *J Biol Chem* **293**: 18636–18645.  
26  
27  
28 617 Bolger AM, Lohse M, Usadel B. 2014. Trimmomatic: a flexible trimmer for Illumina  
29 618 sequence data. *Bioinformatics* **30**: 2114–2120.  
30  
31  
32 619 Bonchi C, Imperi F, Minandri F, Visca P, Frangipani E. 2014. Repurposing of gallium-  
33 620 based drugs for antibacterial therapy: Gallium-based antibacterials. *BioFactors* **40**:  
34 621 303–312.  
35  
36  
37 622 Burstein D, Amaro F, Zusman T, Lifshitz Z, Cohen O, Gilbert JA, Pupko T, Shuman HA,  
38 623 Segal G. 2016. Genomic analysis of 38 *Legionella* species identifies large and  
39 624 diverse effector repertoires. *Nat Genet* **48**: 167–175.  
40  
41  
42 625 Bury-Moné S, Mendz GL, Ball GE, Thibonnier M, Stingl K, Ecobichon C, Avé P, Huerre  
43 626 M, Labigne A, Thiberge J-M, et al. 2008. Roles of alpha and beta carbonic  
44 627 anhydrases of *Helicobacter pylori* in the urease-dependent response to acidity and  
45 628 in colonization of the murine gastric mucosa. *Infect Immun* **76**: 497–509.  
46  
47  
48 629 Chan PP, Lowe TM. 2019. TRNAscan-SE: Searching for tRNA genes in genomic  
49 630 sequences. *Methods Mol Biol* **1962**: 1–14.  
50  
51  
52  
53  
54  
55  
56  
57  
58  
59  
60

- 1  
2  
3 631 Chen C, Banga S, Mertens K, Weber MM, Gorbaslieva I, Tan Y, Luo Z-Q, Samuel JE.  
4 632 2010. Large-scale identification and translocation of type IV secretion substrates  
5 633 by *Coxiella burnetii*. *Proc Natl Acad Sci U S A* **107**: 21755–21760.  
6  
7  
8 634 Chong RA, Moran NA. 2018. Evolutionary loss and replacement of *Buchnera*, the  
9 635 obligate endosymbiont of aphids. *ISME J* **12**: 898–908.  
10  
11  
12 636 Clifford CM, Hoogstraal H, Radovsky FJ, Stiller D, Keirans JE. 1980. *Ornithodoros*  
13 637 (*Alectorobius*) *amblus* (Acarina: Ixodoidea: Argasidae): identity, marine bird and  
14 638 human hosts, virus infections, and distribution in Peru. *J Parasitol* **66**: 312–323.  
15  
16  
17 639 Cohen O, Ashkenazy H, Belinky F, Huchon D, Pupko T. 2010. GLOOME: gain loss  
18 640 mapping engine. *Bioinformatics* **26**: 2914–2915.  
19  
20  
21 641 Coleman J. 1990. Characterization of *Escherichia coli* cells deficient in 1-acyl-sn-glycerol-  
22 642 3- phosphate acyltransferase activity. *J Biol Chem* **265**: 17215–17221.  
23  
24  
25 643 Cox HR. 1938. A filter-passing infectious agent isolated from ticks: III. Description of  
26 644 organism and cultivation experiments. *Public Health Rep* **53**: 2270–2276.  
27  
28  
29 645 Darriba D, Taboada GL, Doallo R, Posada D. 2012. jModelTest 2: more models, new  
30 646 heuristics and parallel computing. *Nat Methods* **9**: 772–772.  
31  
32  
33 647 Duarte RT, Carvalho Simões MC, Sgarbieri VC. 1999. Bovine blood components:  
34 648 fractionation, composition, and nutritive value. *J. Agric. Food Chem.* **47**:231–236.  
35  
36  
37 649 Duron O, Binetruy F, Noël V, Cremaschi J, McCoy KD, Arnathau C, Plantard O,  
38 650 Goolsby J, Pérez de León AA, Heylen DJA, et al. 2017. Evolutionary changes in  
39 651 symbiont community structure in ticks. *Mol Ecol* **26**: 2905–2921.  
40  
41  
42 652 Duron O, Gottlieb Y. 2020. Convergence of nutritional symbioses in obligate blood  
43 653 feeders. *Trends Parasitol* **36**: 816–825.  
44  
45  
46 654 Duron O, Morel O, Noël V, Buysse M, Binetruy F, Lancelot R, Loire E, Ménard C,  
47 655 Bouchez O, Vavre F, et al. 2018. Tick-bacteria mutualism depends on B vitamin  
48 656 synthesis pathway. *Curr Biol* **28**: 1896-1902.e5.  
49  
50  
51 657 Duron O, Noël V, McCoy KD, Bonazzi M, Sidi-Boumedine K, Morel O, Vavre F, Zenner  
52 658 L, Jourdain E, Durand P, et al. 2015a. The recent evolution of a maternally-  
53 659 inherited endosymbiont of ticks led to the emergence of the Q fever pathogen,  
54 660 *Coxiella burnetii*. *PLoS Pathog* **11**: e1004892.  
55  
56  
57  
58  
59  
60

- 1  
2  
3 661 Duron O, Sidi-Boumedine K, Rousset E, Moutailler S, Jourdain E. 2015b. The  
4 662 importance of ticks in Q fever transmission: What has (and has not) been  
5 663 demonstrated? *Trends Parasitol* **31**: 536–552.  
6  
7  
8 664 Eldin C, Mélenotte C, Mediannikov O, Ghigo E, Million M, Edouard S, Mege J-L,  
9 665 Maurin M, Raoult D. 2017. From Q fever to *Coxiella burnetii* infection: A  
10 666 paradigm change. *Clin Microbiol Rev* **30**: 115–190.  
11  
12  
13 667 Elliman JR, Owens L. 2020. Confirmation that *candidatus* *Coxiella cheraxi* from redclaw  
14 668 crayfish (*Cherax quadricarinatus*) is a close relative of *Coxiella burnetii*, the agent of  
15 669 Q-fever. *Lett Appl Microbiol* **71**: 320–326.  
16  
17  
18 670 Emms DM, Kelly S. 2015. OrthoFinder: solving fundamental biases in whole genome  
19 671 comparisons dramatically improves orthogroup inference accuracy. *Genome Biol*  
20 672 **16**: 157.  
21  
22  
23 673 Endley S, McMurray D, Ficht TA. 2001. Interruption of the *cydB* locus in *Brucella abortus*  
24 674 attenuates intracellular survival and virulence in the mouse model of infection. *J*  
25 675 *Bacteriol* **183**: 2454–2462.  
26  
27  
28 676 Gerhart JG, Dutcher HA, Brenner AE, Moses AS, Grubhoffer L, Raghavan R. 2018.  
29 677 Multiple acquisitions of pathogen-derived *Francisella* endosymbionts in soft ticks.  
30 678 *Genome Biol Evol* **10**: 607–615.  
31  
32  
33 679 Gerhart JG, Moses AS, Raghavan R. 2016. A *Francisella*-like endosymbiont in the Gulf  
34 680 Coast tick evolved from a mammalian pathogen. *Sci Rep* **6**: 33670.  
35  
36  
37 681 Gilk SD. 2012. Role of lipids in *Coxiella burnetii* infection. *Adv Exp Med Biol* **984**: 199–213.  
38  
39  
40 682 Gilk SD, Beare PA, Heinzen RA. 2010. *Coxiella burnetii* expresses a functional  $\Delta 24$  sterol  
41 683 reductase. *J Bacteriol* **192**: 6154–6159.  
42  
43  
44 684 Goss CH, Kaneko Y, Khuu L, Anderson GD, Ravishankar S, Aitken ML, Lechtzin N,  
45 685 Zhou G, Czyz DM, McLean K, et al. 2018. Gallium disrupts bacterial iron  
46 686 metabolism and has therapeutic effects in mice and humans with lung infections.  
47 687 *Sci Transl Med* **10**: eaat7520.  
48  
49  
50 688 Gottlieb Y, Lalzar I, Klasson L. 2015. Distinctive genome reduction rates revealed by  
51 689 genomic analyses of two *Coxiella*-like endosymbionts in ticks. *Genome Biol Evol* **7**:  
52 690 1779–1796.  
53  
54  
55  
56  
57  
58  
59  
60

- 1  
2  
3 691 Guimard T, Amrane S, Prudent E, El Karkouri K, Raoult D, Angelakis E. 2017. Case  
4 692 report: Scalp eschar and neck lymphadenopathy associated with bacteremia due  
5 693 to *Coxiella*-like bacteria. *Am J Trop Med Hyg* **97**: 1319–1322.  
6  
7  
8 694 Guizzo MG, Parizi LF, Nunes RD, Schama R, Albano RM, Tirloni L, Oldiges DP, Vieira  
9 695 RP, Oliveira WHC, Leite M de S, et al. 2017. A *Coxiella* mutualist symbiont is  
10 696 essential to the development of *Rhipicephalus microplus*. *Sci Rep* **7**: 17554.  
11  
12  
13 697 Hackstadt T. 1983. Estimation of the cytoplasmic pH of *Coxiella burnetii* and effect of  
14 698 substrate oxidation on proton motive force. *J Bacteriol* **154**: 591–597.  
15  
16  
17 699 Hijazi S, Visaggio D, Pirolo M, Frangipani E, Bernstein L, Visca P. 2018. Antimicrobial  
18 700 activity of gallium compounds on ESKAPE pathogens. *Front Cell Infect Microbiol*  
19 701 **8**: 316.  
20  
21  
22 702 Hijazi S, Visca P, Frangipani E. 2017. Gallium-protoporphyrin IX inhibits *Pseudomonas*  
23 703 *aeruginosa* growth by targeting cytochromes. *Front Cell Infect Microbiol* **7**: 12.  
24  
25  
26 704 Hill J, Samuel JE. 2011. *Coxiella burnetii* acid phosphatase inhibits the release of reactive  
27 705 oxygen intermediates in polymorphonuclear leukocytes. *Infect Immun* **79**: 414–  
28 706 420.  
29  
30  
31 707 Hosokawa T, Koga R, Kikuchi Y, Meng X-Y, Fukatsu T. 2010. *Wolbachia* as a  
32 708 bacteriocyte-associated nutritional mutualist. *Proc Natl Acad Sci* **107**: 769–774.  
33  
34  
35 709 Hyatt D, Chen G-L, LoCascio PF, Land ML, Larimer FW, Hauser LJ. 2010. Prodigal:  
36 710 prokaryotic gene recognition and translation initiation site identification. *BMC*  
37 711 *Bioinformatics* **11**: 119.  
38  
39  
40 712 Iwata-Reuyl D. 2003. Biosynthesis of the 7-deazaguanosine hypermodified nucleosides  
41 713 of transfer RNA. *Bioorganic Chem* **31**: 24–43.  
42  
43  
44 714 Jansen R, Bussemaker HJ, Gerstein M. 2003. Revisiting the codon adaptation index from  
45 715 a whole-genome perspective: analyzing the relationship between gene  
46 716 expression and codon occurrence in yeast using a variety of models. *Nucleic Acids*  
47 717 *Res* **31**: 2242–2251.  
48  
49  
50 718 Katoh K, Standley DM. 2013. MAFFT multiple sequence alignment software version 7:  
51 719 improvements in performance and usability. *Mol Biol Evol* **30**: 772–780.  
52  
53  
54  
55  
56  
57  
58  
59  
60

- 1  
2  
3 720 Klyachko O, Stein BD, Grindle N, Clay K, Fuqua C. 2007. Localization and visualization  
4 721 of a *Coxiella*-type symbiont within the lone star tick, *Amblyomma americanum*.  
5 722 *Appl Environ Microbiol* **73**: 6584–6594.  
6  
7  
8 723 Koh CS, Sarin LP. 2018. Transfer RNA modification and infection – Implications for  
9 724 pathogenicity and host responses. *Biochim Biophys Acta Gene Regul Mech* **1861**:  
10 725 419–432.  
11  
12  
13 726 Körner S, Makert GR, Mertens-Scholz K, Henning K, Pfeffer M, Starke A, Nijhof AM,  
14 727 Ulbert S. 2020. Uptake and fecal excretion of *Coxiella burnetii* by *Ixodes ricinus* and  
15 728 *Dermacentor marginatus* ticks. *Parasit Vectors* **13**: 75.  
16  
17  
18 729 Kozlowski LP. 2016. IPC – Isoelectric Point Calculator. *Biol Direct* **11**: 55.  
19  
20  
21 730 Kuba M, Neha N, Newton P, Lee YW, Bennett-Wood V, Hachani A, De Souza DP,  
22 731 Nijagal B, Dayalan S, Tull D, et al. 2020. EirA is a novel protein essential for  
23 732 intracellular replication of *Coxiella burnetii*. *Infect Immun* **88**.  
24  
25  
26 733 Lagesen K, Hallin P, Rødland EA, Stærfeldt H-H, Rognes T, Ussery DW. 2007.  
27 734 RNAMmer: consistent and rapid annotation of ribosomal RNA genes. *Nucleic*  
28 735 *Acids Res* **35**: 3100–3108.  
29  
30  
31 736 Lawrence JG, Ochman H. 1997. Amelioration of bacterial genomes: rates of change and  
32 737 exchange. *J Mol Evol* **44**: 383–397.  
33  
34  
35 738 Lerat E, Daubin V, Ochman H, Moran NA. 2005. Evolutionary origins of genomic  
36 739 repertoires in bacteria. *PLoS Biol* **3**: e130.  
37  
38  
39 740 Li L-H, Zhang Y, Zhu D. 2018. Effects of antibiotic treatment on the fecundity of  
40 741 *Rhipicephalus haemaphysaloides* ticks. *Parasit Vectors* **11**.  
41  
42  
43 742 Martinez E, Cantet F, Fava L, Norville I, Bonazzi M. 2014. Identification of OmpA, a  
44 743 *Coxiella burnetii* protein involved in host cell invasion, by multi-phenotypic high-  
45 744 content screening. *PLoS Pathog* **10**: e1004013.  
46  
47  
48 745 Martinez E, Huc-Brandt S, Brelle S, Allombert J, Cantet F, Gannoun-Zaki L, Burette M,  
49 746 Martin M, Letourneur F, Bonazzi M, et al. 2020. The secreted protein kinase CstK  
50 747 from *Coxiella burnetii* influences vacuole development and interacts with the  
51 748 GTPase-activating host protein TBC1D5. *J Biol Chem* **295**: 7391–7403.  
52  
53  
54  
55  
56  
57  
58  
59  
60

- 1  
2  
3 749 Maturana P, Graham JG, Sharma UM, Voth DE. 2013. Refining the plasmid-encoded  
4 750 type IV secretion system substrate repertoire of *Coxiella burnetii*. *J Bacteriol* **195**:  
5 751 3269–3276.  
6  
7  
8 752 Maurin M, Raoult D. 1999. Q Fever. *Clin Microbiol Rev* **12**: 518–553.  
9  
10  
11 753 McCutcheon JP, Moran NA. 2011. Extreme genome reduction in symbiotic bacteria. *Nat*  
12 754 *Rev Microbiol* **10**: 13–26.  
13  
14  
15 755 McCutcheon JP, Moran NA. 2010. Functional convergence in reduced genomes of  
16 756 bacterial symbionts spanning 200 My of evolution. *Genome Biol Evol* **2**: 708–718.  
17  
18  
19 757 Mertens K, Samuel JE. 2012. Defense mechanisms against oxidative stress in *Coxiella*  
20 758 *burnetii*: adaptation to a unique intracellular niche. *Adv Exp Med Biol* **984**: 39–63.  
21  
22  
23 759 Moran NA. 2002. Microbial minimalism: genome reduction in bacterial pathogens. *Cell*  
24 760 **108**: 583–586.  
25  
26  
27 761 Moran NA, Munson MA, Baumann P, Ishikawa H. 1993. A molecular clock in  
28 762 endosymbiotic bacteria is calibrated using the insect hosts. *Proc Biol Sci* **253**: 167–  
29 763 171.  
30  
31  
32 764 Moses AS, Millar JA, Bonazzi M, Beare PA, Raghavan R. 2017. Horizontally acquired  
33 765 biosynthesis genes boost *Coxiella burnetii*'s physiology. *Front Cell Infect Microbiol*  
34 766 **7**: 174.  
35  
36  
37 767 Nakabachi A, Yamashita A, Toh H, Ishikawa H, Dunbar HE, Moran NA, Hattori M.  
38 768 2006. The 160-kilobase genome of the bacterial endosymbiont *Carsonella*. *Science*  
39 769 **314**: 267.  
40  
41  
42 770 Needle DB, Agnew DW, Bradway DS, Nordhausen RW, Garner MM. 2020. Avian  
43 771 coxiellosis in nine psittacine birds, one black-browed barbet, and one paradise  
44 772 tanager. *Avian Pathol J WVPA* **49**: 268–274.  
45  
46  
47 773 Newton HJ, Kohler LJ, McDonough JA, Temoche-Diaz M, Crabill E, Hartland EL, Roy  
48 774 CR. 2014. A screen of *Coxiella burnetii* mutants reveals important roles for  
49 775 Dot/Icm effectors and host autophagy in vacuole biogenesis. *PLOS Pathog* **10**:  
50 776 e1004286.  
51  
52  
53  
54 777 Neyrolles O, Wolschendorf F, Mitra A, Niederweis M. 2015. *Mycobacteria*, metals, and  
55 778 the macrophage. *Immunol Rev* **264**: 249–263.  
56  
57  
58  
59  
60

- 1  
2  
3 779 Nurk S, Meleshko D, Korobeynikov A, Pevzner PA. 2017. metaSPAdes: a new versatile  
4 780 metagenomic assembler. *Genome Res* **27**: 824–834.  
5  
6  
7 781 Ochman H, Lawrence JG, Groisman EA. 2000. Lateral gene transfer and the nature of  
8 782 bacterial innovation. *Nature* **405**: 299–304.  
9  
10  
11 783 Omsland A, Heinzen RA. 2011. Life on the outside: the rescue of *Coxiella burnetii* from  
12 784 its host cell. *Annu Rev Microbiol* **65**: 111–128.  
13  
14  
15 785 Peer A, Margalit H. 2014. Evolutionary patterns of *Escherichia coli* small RNAs and their  
16 786 regulatory interactions. *RNA* **20**: 994–1003.  
17  
18  
19 787 Potter SC, Luciani A, Eddy SR, Park Y, Lopez R, Finn RD. 2018. HMMER web server:  
20 788 2018 update. *Nucleic Acids Res* **46**: W200–W204.  
21  
22  
23 789 Perotti MA, Allen JM, Reed DL, Braig HR. 2007. Host-symbiont interactions of the  
24 790 primary endosymbiont of human head and body lice. *FASEB J* **21**: 1058–1066.  
25  
26  
27 791 Raghavan R, Kelkar YD, Ochman H. 2012. A selective force favoring increased G+C  
28 792 content in bacterial genes. *Proc Natl Acad Sci U S A* **109**: 14504–14507.  
29  
30  
31 793 Ronquist F, Teslenko M, van der Mark P, Ayres DL, Darling A, Höhna S, Larget B, Liu  
32 794 L, Suchard MA, Huelsenbeck JP. 2012. MrBayes 3.2: efficient Bayesian  
33 795 phylogenetic inference and model choice across a large model space. *Syst Biol* **61**:  
34 796 539–542.  
35  
36  
37 797 Rowland JL, Niederweis M. 2012. Resistance mechanisms of *Mycobacterium tuberculosis*  
38 798 against phagosomal copper overload. *Tuberc Edinb Scotl* **92**: 202–210.  
39  
40  
41 799 Rowlett VW, Mallampalli VKPS, Karlstaedt A, Dowhan W, Taegtmeier H, Margolin W,  
42 800 Vitrac H. 2017. Impact of membrane phospholipid alterations in *Escherichia coli*  
43 801 on cellular function and bacterial stress adaptation. *J Bacteriol* **199**: e00849-16.  
44  
45  
46 802 Russell JA, Oliver KM, Hansen AK. 2017. Band-aids for *Buchnera* and B vitamins for all.  
47 803 *Mol Ecol* **26**: 2199–2203.  
48  
49  
50 804 Saiki K, Mogi T, Anraku Y. 1992. Heme O biosynthesis in *Escherichia coli*: the *cyoE* gene  
51 805 in the cytochrome bo operon encodes a protoheme IX farnesyltransferase.  
52 806 *Biochem Biophys Res Commun* **189**: 1491–1497.  
53  
54  
55  
56  
57  
58  
59  
60

- 1  
2  
3 807 Samanta D, Clemente TM, Schuler BE, Gilk SD. 2019. *Coxiella burnetii* type 4B secretion  
4 808 system-dependent manipulation of endolysosomal maturation is required for  
5 809 bacterial growth. *PLoS Pathog* **15**: e1007855.  
6  
7  
8 810 Sanchez SE, Omsland A. 2020. Critical role for molecular iron in *Coxiella burnetii*  
9 811 replication and viability. *mSphere* **5**: e00458-20.  
10  
11  
12 812 Sandoz KM, Popham DL, Beare PA, Sturdevant DE, Hansen B, Nair V, Heinzen RA.  
13 813 2016. Transcriptional profiling of *Coxiella burnetii* reveals extensive cell wall  
14 814 remodeling in the small cell variant developmental form. *PloS One* **11**: e0149957.  
15  
16  
17 815 Segal G, Russo JJ, Shuman HA. 1999. Relationships between a new type IV secretion  
18 816 system and the icm/dot virulence system of *Legionella pneumophila*. *Mol Microbiol*  
19 817 **34**: 799–809.  
20  
21  
22 818 Seo M-G, Lee S-H, VanBik D, Ouh I-O, Yun S-H, Choi E, Park Y-S, Lee S-E, Kim JW,  
23 819 Cho G-J, et al. 2016. Detection and genotyping of *Coxiella burnetii* and *Coxiella*-like  
24 820 bacteria in horses in South Korea. *PloS One* **11**: e0156710.  
25  
26  
27 821 Seshadri R, Paulsen IT, Eisen JA, Read TD, Nelson KE, Nelson WC, Ward NL, Tettelin  
28 822 H, Davidsen TM, Beanan MJ, et al. 2003. Complete genome sequence of the Q-  
29 823 fever pathogen *Coxiella burnetii*. *Proc Natl Acad Sci U S A* **100**: 5455–5460.  
30  
31  
32 824 Sharp PM, Li WH. 1987. The codon adaptation index--a measure of directional  
33 825 synonymous codon usage bias, and its potential applications. *Nucleic Acids Res*  
34 826 **15**: 1281–1295.  
35  
36  
37 827 Shivaprasad HL, Cadenas MB, Diab SS, Nordhausen R, Bradway D, Crespo R,  
38 828 Breitschwerdt EB. 2008. *Coxiella*-like infection in psittacines and a toucan. *Avian*  
39 829 *Dis* **52**: 426–432.  
40  
41  
42 830 Smith DJW, Derrick EH. 1940. Studies in the epidemiology of Q fever: 1. The isolation of  
43 831 six strains of *Rickettsia burneti* from the tick *Haemaphysalis humerosa*. *Aust J Exp*  
44 832 *Biol Med Sci* **18**: 1–8.  
45  
46  
47 833 Smith TA, Driscoll T, Gillespie JJ, Raghavan R. 2015. A *Coxiella*-like endosymbiont is a  
48 834 potential vitamin source for the Lone Star tick. *Genome Biol Evol* **7**: 831–838.  
49  
50  
51 835 Stamatakis A. 2014. RAxML version 8: a tool for phylogenetic analysis and post-analysis  
52 836 of large phylogenies. *Bioinformatics* **30**: 1312–1313.  
53  
54  
55  
56  
57  
58  
59  
60



- 1  
2  
3 837 Stead CM, Cockrell DC, Beare PA, Miller HE, Heinzen RA. 2018. A *Coxiella burnetii*  
4 838 phospholipase A homolog *pldA* is required for optimal growth in macrophages  
5 839 and developmental form lipid remodeling. *BMC Microbiol* **18**: 33.  
6  
7  
8 840 Sterkel M, Oliveira JHM, Bottino-Rojas V, Paiva-Silva GO, Oliveira PL. 2017. The dose  
9 841 makes the poison: Nutritional overload determines the life traits of blood-feeding  
10 842 arthropods. *Trends Parasitol.* **33**:633–644.  
11  
12  
13 843 Stojiljkovic I, Kumar V, Srinivasan N. 1999. Non-iron metalloporphyrins: potent  
14 844 antibacterial compounds that exploit haem/Hb uptake systems of pathogenic  
15 845 bacteria. *Mol Microbiol* **31**: 429–442.  
16  
17  
18  
19 846 Talavera G, Castresana J. 2007. Improvement of phylogenies after removing divergent  
20 847 and ambiguously aligned blocks from protein sequence alignments. *Syst Biol* **56**:  
21 848 564–577.  
22  
23  
24 849 Tsementzi D, Castro Gordillo J, Mahagna M, Gottlieb Y, Konstantinidis KT. 2018.  
25 850 Comparison of closely related, uncultivated *Coxiella* tick endosymbiont  
26 851 population genomes reveals clues about the mechanisms of symbiosis. *Environ*  
27 852 *Microbiol* **20**: 1751–1764.  
28  
29  
30  
31 853 Vallejo Esquerra E, Yang H, Sanchez SE, Omsland A. 2017. Physicochemical and  
32 854 nutritional requirements for axenic replication suggest physiological basis for  
33 855 *Coxiella burnetii* niche restriction. *Front Cell Infect Microbiol* **7**: 190.  
34  
35  
36 856 Wachter S, Bonazzi M, Shifflett K, Moses AS, Raghavan R, Minnick MF. 2019. A CsrA-  
37 857 binding, *trans*-acting sRNA of *Coxiella burnetii* is necessary for optimal  
38 858 intracellular growth and vacuole formation during early infection of host cells. *J*  
39 859 *Bacteriol* **201**: e00524-19.  
40  
41  
42  
43 860 Warriar I, Hicks LD, Battisti JM, Raghavan R, Minnick MF. 2014. Identification of novel  
44 861 small RNAs and characterization of the 6S RNA of *Coxiella burnetii*. *PLoS One* **9**:  
45 862 e100147.  
46  
47  
48 863 Wernegreen JJ, Ochman H, Jones IB, Moran NA. 2000. Decoupling of genome size and  
49 864 sequence divergence in a symbiotic bacterium. *J Bacteriol* **182**: 3867–3869.  
50  
51  
52 865 Woc-Colburn AM, Garner MM, Bradway D, West G, D'Agostino J, Trupkiewicz J, Barr  
53 866 B, Anderson SE, Rurangirwa FR, Nordhausen RW. 2008. Fatal coxiellosis in  
54 867 Swainson's Blue Mountain Rainbow Lorikeets (*Trichoglossus haematodus*  
55 868 *moluccanus*). *Vet Pathol* **45**: 247–254.  
56  
57  
58  
59  
60

1  
2  
3 869 Zhang C-M, Li N-X, Zhang T-T, Qiu Z-X, Li Y, Li L-W, Liu J-Z. 2017. Endosymbiont  
4 870 CLS-HI plays a role in reproduction and development of *Haemaphysalis*  
5 871 *longicornis*. *Exp Appl Acarol* **73**: 429–438.

6  
7  
8 872 Zhong J, Jasinskas A, Barbour AG. 2007. Antibiotic treatment of the tick vector  
9 873 *Amblyomma americanum* reduced reproductive fitness. *PLoS One* **2**: e405.

10  
11  
12 874  
13  
14  
15  
16  
17  
18  
19  
20  
21  
22  
23  
24  
25  
26  
27  
28  
29  
30  
31  
32  
33  
34  
35  
36  
37  
38  
39  
40  
41  
42  
43  
44  
45  
46  
47  
48  
49  
50  
51  
52  
53  
54  
55  
56  
57  
58  
59  
60

875 **Table 1.** Genome characteristics of CLEOA, *C. burnetii*, and CRt

876

	<b>CLEOA</b>	<b><i>C. burnetii</i> RSA493</b>	<b>CRt</b>
NCBI Accession	VFIV00000000	AE016828.3	NZ_CP011126.1
Length (bp)	1,561,173	1,995,488	1,733,840
%GC	40.6	42.7	38.2
rRNA (5S, 16S, 23S)	1,1,1	1,1,1	1,1,1
tRNA	42	42	48
Functional genes	889	1,798	926
Pseudogenes	660	197	383
Single copy genes <sup>a</sup>	106/111	106/111	105/111

877 <sup>a</sup> Albertson et al. 2013

878

879

1  
2  
3 **880 FIGURE LEGENDS**  
4

5  
6 **881 Figure 1. CLEOA is the closet relative of *C. burnetii*.** Maximum likelihood and  
7  
8  
9 **882** Bayesian trees built using 117 single-copy protein-coding genes were combined to  
10  
11 **883** generate the shown phylogenomic tree. Bootstrap support and posterior probabilities  
12  
13 **884** agreed at all branchpoints and are depicted as a single confidence value. The Dot/Icm  
14  
15  
16 **885** Type IVB secretion system (T4BSS), which is critical to pathogenesis, is found in all  
17  
18 **886** members of the order Legionellales, but has been pseudogenized in CLEs. Nodes N1-  
19  
20 **887** N5 mark major branching points in the evolution of *C. burnetii*.  
21  
22  
23  
24

25 **888**

26  
27 **889 Figure 2. CLEs contain nonfunctional T4BSS.** Comparison of T4BSS genes in CLEOA,  
28  
29 **890** *C. burnetii* RSA493 and CRT indicate that the secretion system has been rendered  
30  
31 **891** nonfunctional in tick endosymbionts. Filled blocks represent intact genes. Outlined  
32  
33 **892** blocks represent pseudogenized genes.  
34  
35  
36  
37

38 **893**

39  
40 **894 Figure 3. CLE clades contain both tick endosymbionts and pathogens.** A 16S rDNA-  
41  
42 **895** based phylogenetic tree is shown. Bootstrap support and posterior probabilities are  
43  
44 **896** labeled above and below branchpoints, respectively. Nodes with  $\leq 70\%$  bootstrap  
45  
46 **897** support were collapsed to polytomies. Taxa colors represent the continent from which  
47  
48 **898** the host was derived. Established pathogens are marked with asterisks. Clades A-D  
49  
50 **899** were originally defined by Duron et al. 2015a.  
51  
52  
53  
54  
55  
56  
57  
58  
59  
60

900

**901 Figure 4. HGT was a major contributor to gene accumulation in *C. burnetii*'s****902 ancestors.** Nodes N1-N5 (as labeled in Fig. 1) represent major branchpoints in the903 evolution of *C. burnetii*. (A) and (B) depict %GC and Codon Adaptation Index (CAI)

904 distributions, respectively, for genes originating at each node. Boxes illustrate each

905 distribution's interquartile range while the black line dividing the box represents the

906 median. Whiskers represent minimum and maximum values, excluding outliers (black

907 diamonds) which were determined using the Tukey method. P-values shown in tables

908 are for pairwise T-tests (pooled SD, BKY adjusted). Genes gained at N2 were excluded

909 due to small sample size ( $n=13$ ). (C) *C. burnetii* genome composition based on nodes of

910 gene origin: N1: 43.9%, N2: 0.7%, N3: 8.2%, N4: 22.6%, N5: 8.6%. The unlabeled portion

911 represents potentially spurious genes ( $n=224$ ) as well as genes with undefined nodes of912 origin ( $n=44$ ).

913

**914 Figure 5. CLEs and FLEs encode B vitamin and cofactor biosynthetic pathways.**915 CLEOA, CRt, CLEAA, FLE-Om (*Francisella* endosymbiont of *Ornithodoros moubata*;916 LVCE00000000), FLE-Am (*Francisella* endosymbiont of *Amblyomma maculatum*;917 LNCT00000000), and *F. persica* (FLE in *Argas arboreus*; NZ\_CP013022) contain intact

918 pathways for the synthesis of B vitamins and cofactors. Enzymes catalyzing each step

919 are labeled with gene names and EC numbers. Blocks with no color indicate that a

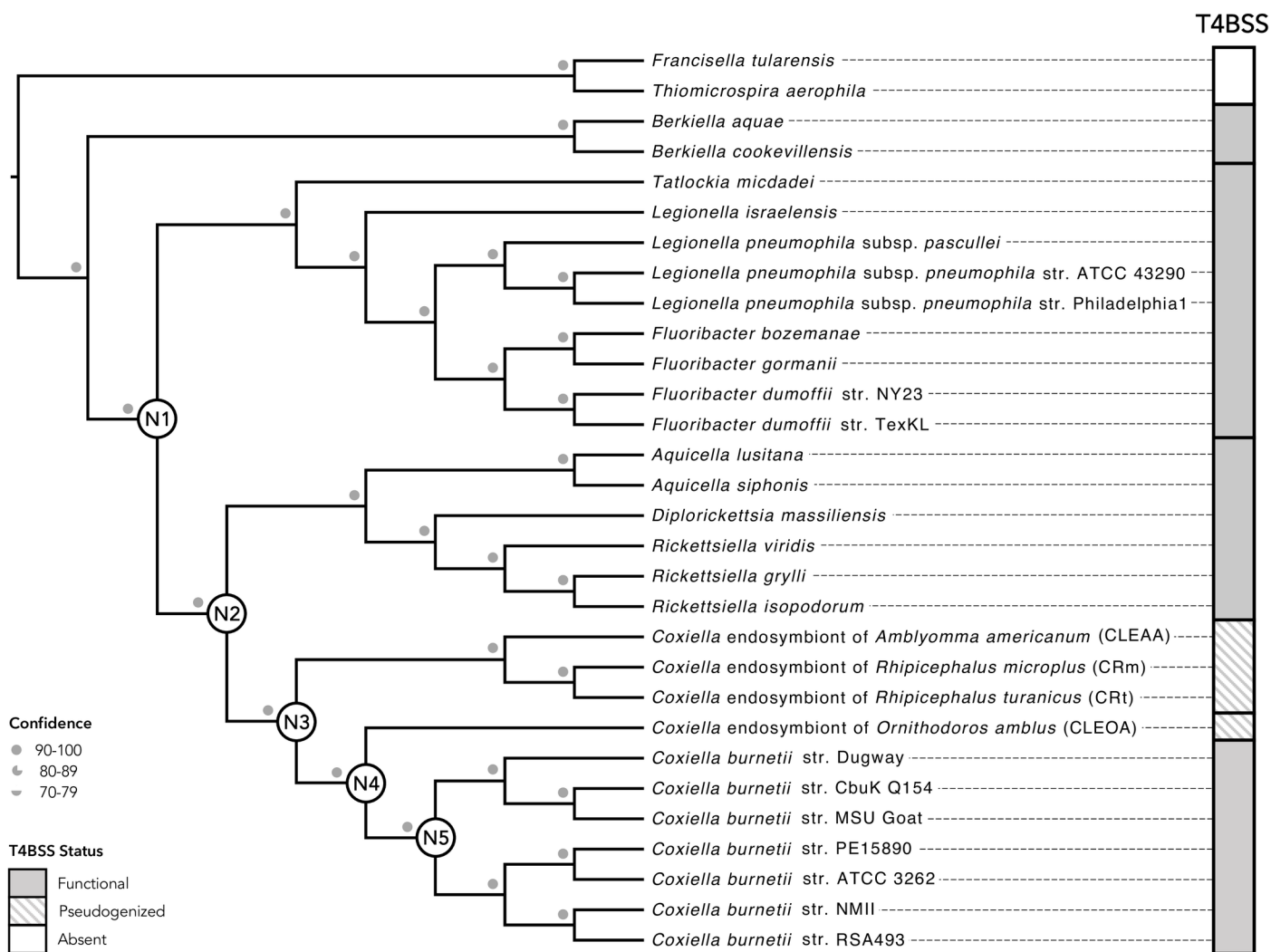
1  
2  
3 920 functional copy of a gene was not detected in that genome. Depictions of metabolic  
4  
5  
6 921 pathways modified from Gerhart et al. 2018.  
7

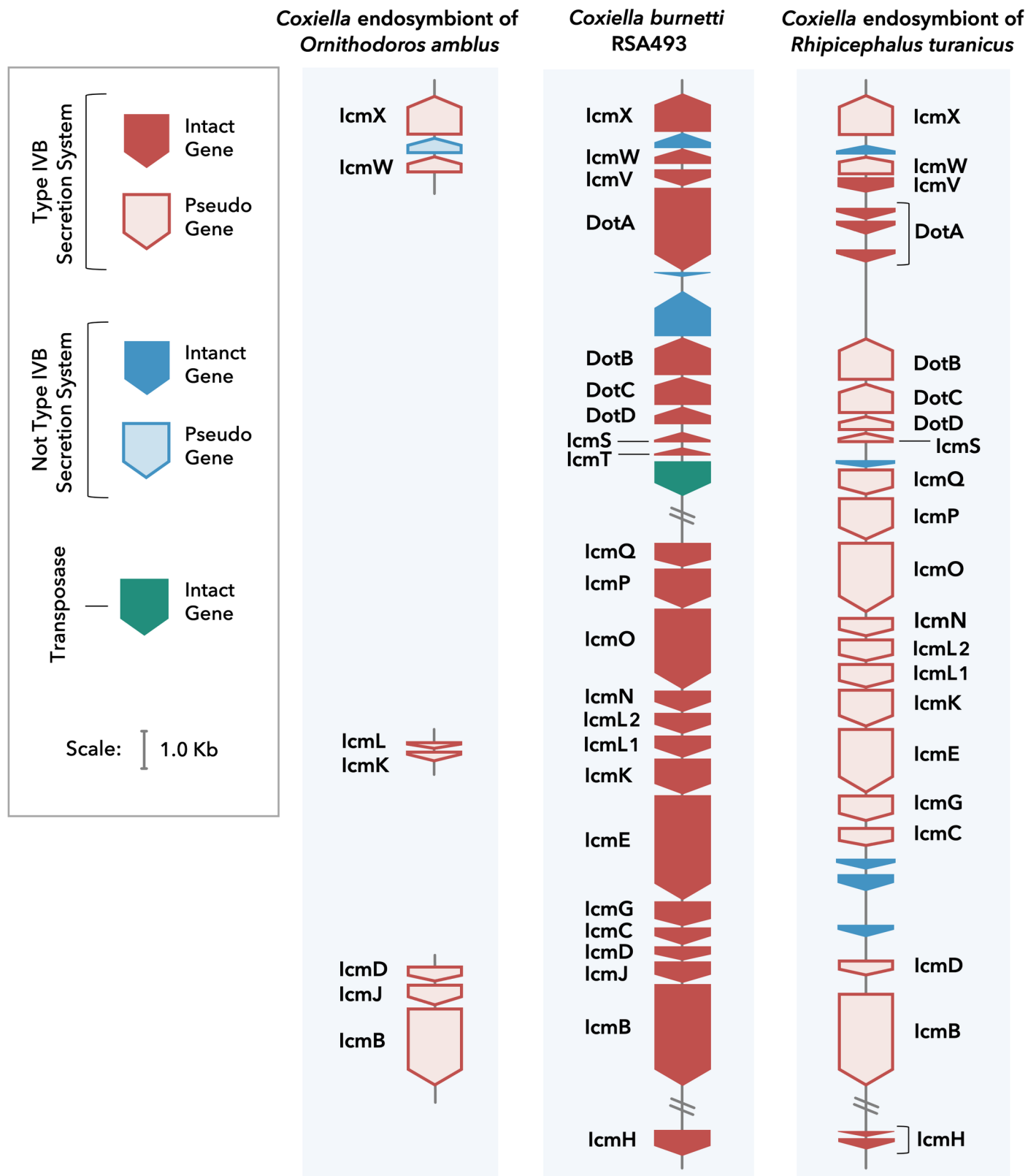
8  
9 922

10  
11 923 **Figure 6. A heme analog reduces *C. burnetii* growth.** (A) Bacteria growing in ACCM-2  
12  
13  
14 924 were exposed to concentrations of GaPPIX shown in x-axis and were quantified using  
15  
16  
17 925 PicoGreen at 8h, 24h, 48h, and 72h post-treatment. Data shown are mean fluorescence  
18  
19  
20 926 intensity ( $\pm$  SE) compared to the vehicle control (0nM). Statistical significance was  
21  
22 927 analyzed using two-way repeated measures ANOVA followed by Dunnett's test (n=5).  
23

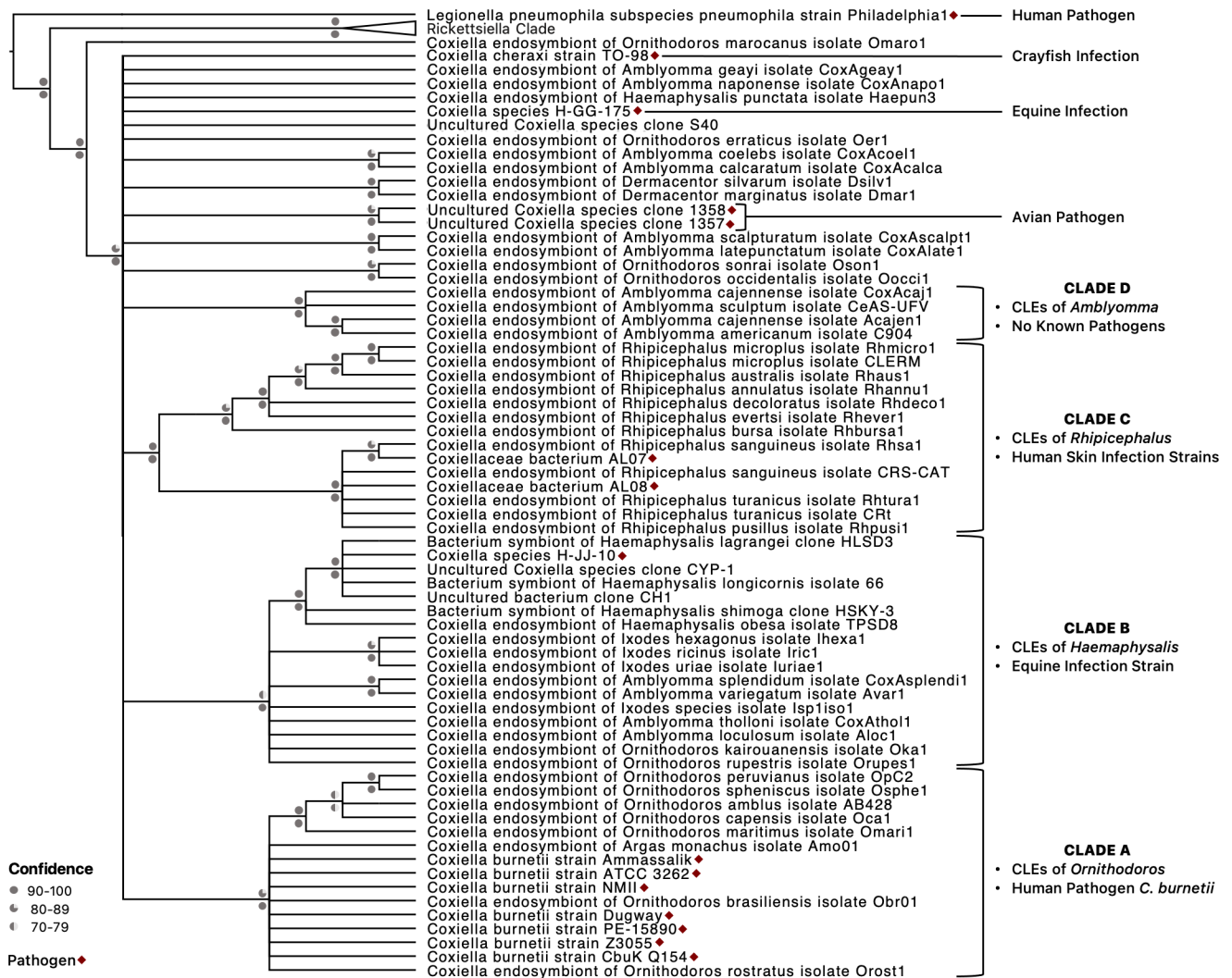
24  
25 928 (B) At 72h post-treatment, bacterial growth within THP-1 cells was quantified using  
26  
27  
28 929 qPCR. Data shown as mean fold difference ( $\pm$  SE) compared to control. (C) At 24h post-  
29  
30  
31 930 GaPPIX treatment of THP-1 cells, lactate dehydrogenase (LDH) activity was determined  
32  
33 931 by measuring the level of resorufin formation using an LDH cytotoxicity assay. The  
34  
35  
36 932 cytotoxicity was reported as the percentage LDH released compared to the maximum  
37  
38  
39 933 LDH activity. Data shown as mean percentage LDH released ( $\pm$  SEM). For both B and C,  
40  
41 934 statistical significance was analyzed using one-way ANOVA followed by Dunnett's test  
42  
43  
44 935 (n=3).  
45

46 936  
47  
48  
49  
50  
51  
52  
53  
54  
55  
56  
57  
58  
59  
60

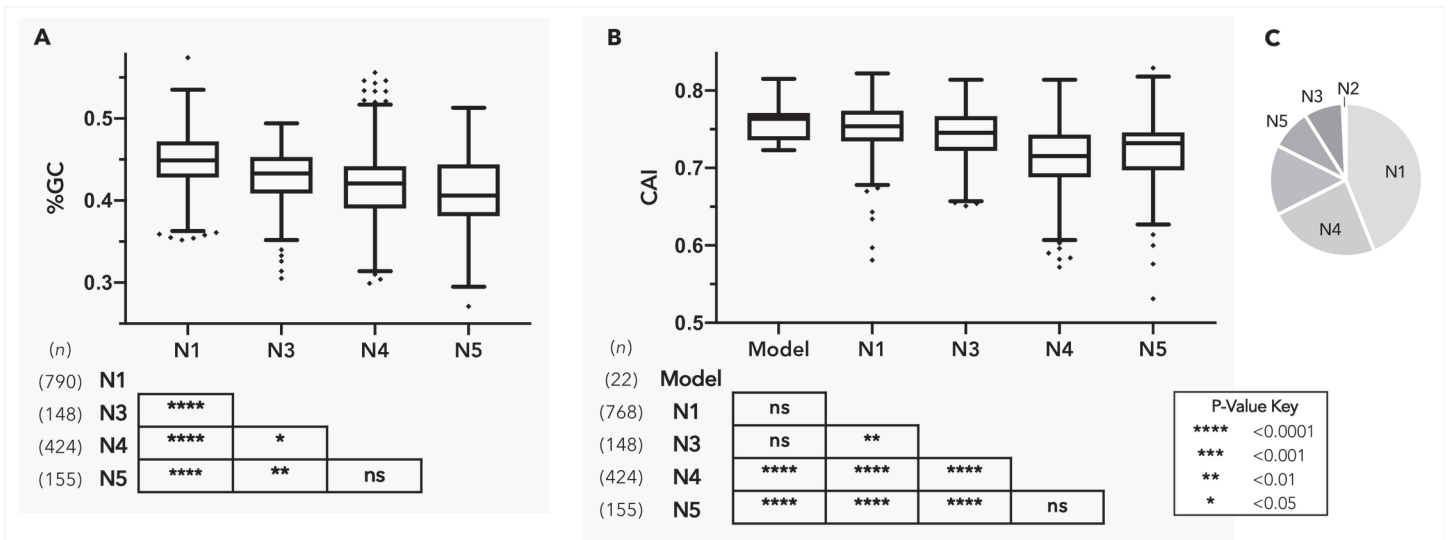


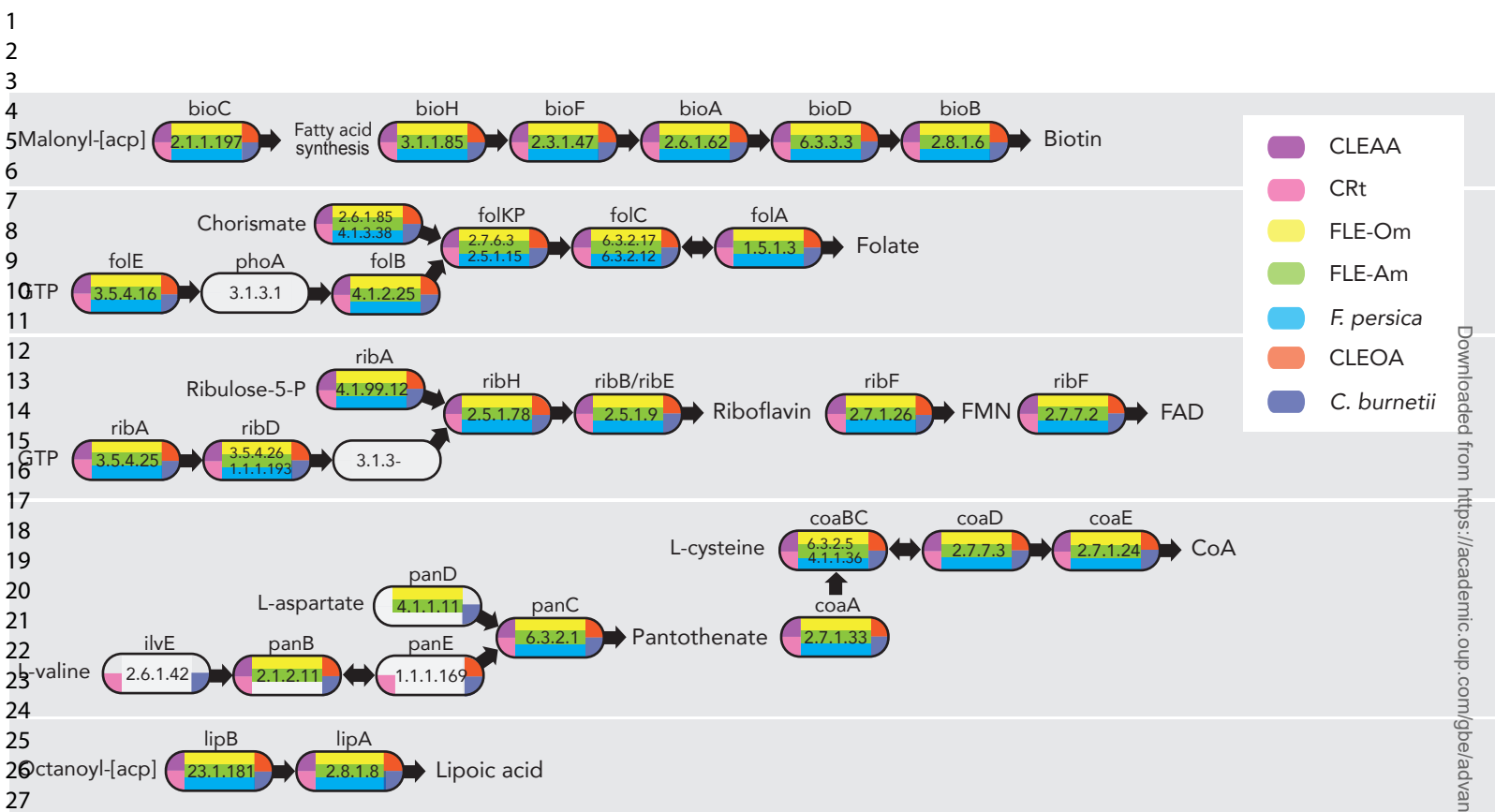






Downloaded from https://academic.oup.com/gbe/advance-article/doi/10.1093/gbe/evab108/6278299 by guest on 26 May 2021





Downloaded from https://academic.oup.com/gbe/advance-article/doi/10.1093/gbe/evab108/6278299 by guest on 26 May 2021

1  
2  
3  
4  
5  
6  
7  
8  
9  
10  
11  
12  
13  
14  
15  
16  
17  
18  
19  
20  
21  
22  
23  
24  
25  
26  
27  
28  
29  
30  
31  
32  
33  
34  
35  
36  
37  
38  
39  
40  
41  
42  
43  
44  
45  
46  
47  
48  
49  
50  
51  
52  
53  
54  
55  
56  
57  
58  
59  
60

